Development of a frozen-spin muon trap for the search for a muon EDM

– SPS Annual Meeting (5 September 2023) –

Tim Hume

Supervised by Dr. Philipp Schmidt-Wellenburg

PAUL SCHERRER INSTITUT

ETH zürich

timothy.hume@psi.ch

muEDM Experiment at PSI

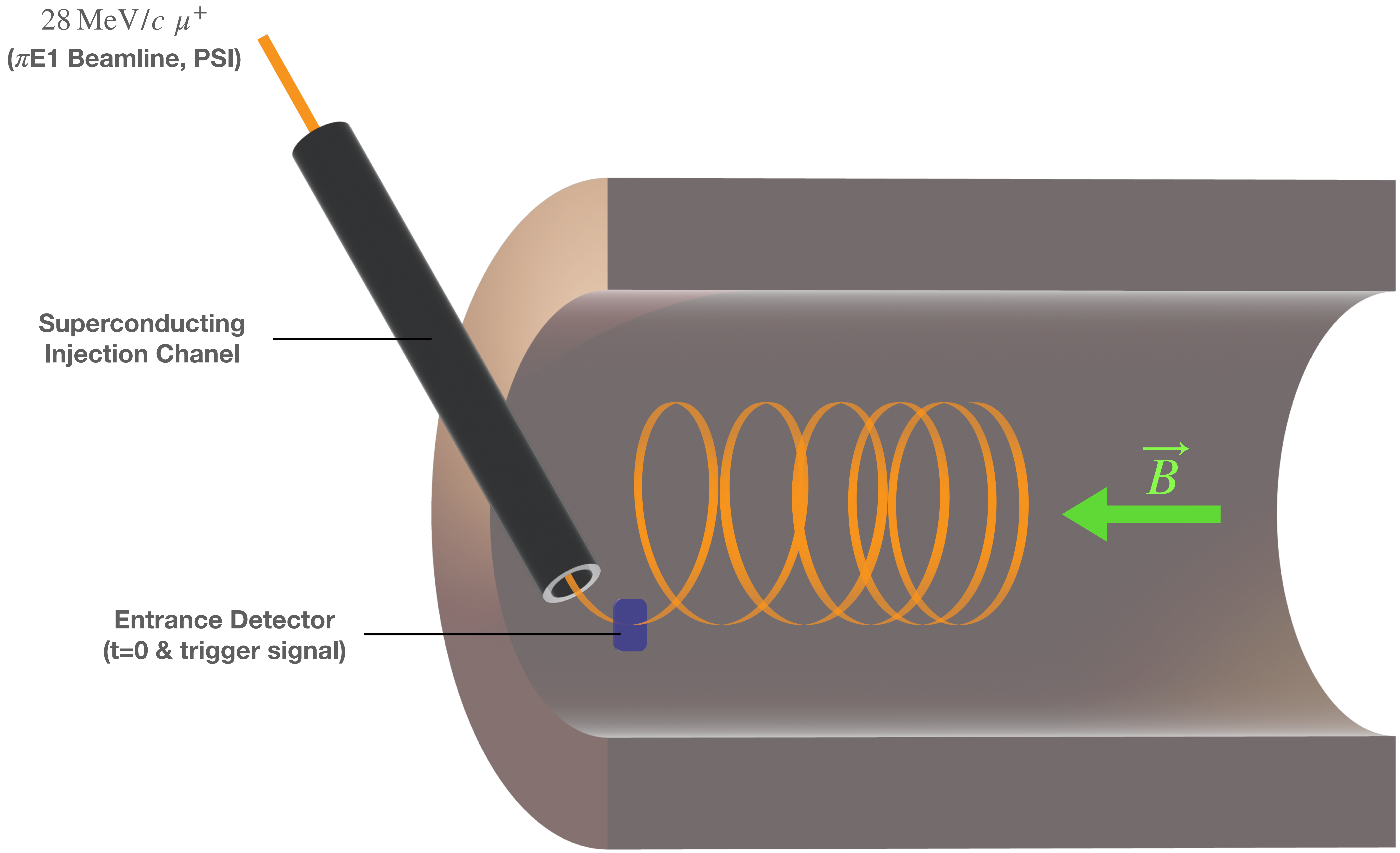

muEDM Experiment at PSI

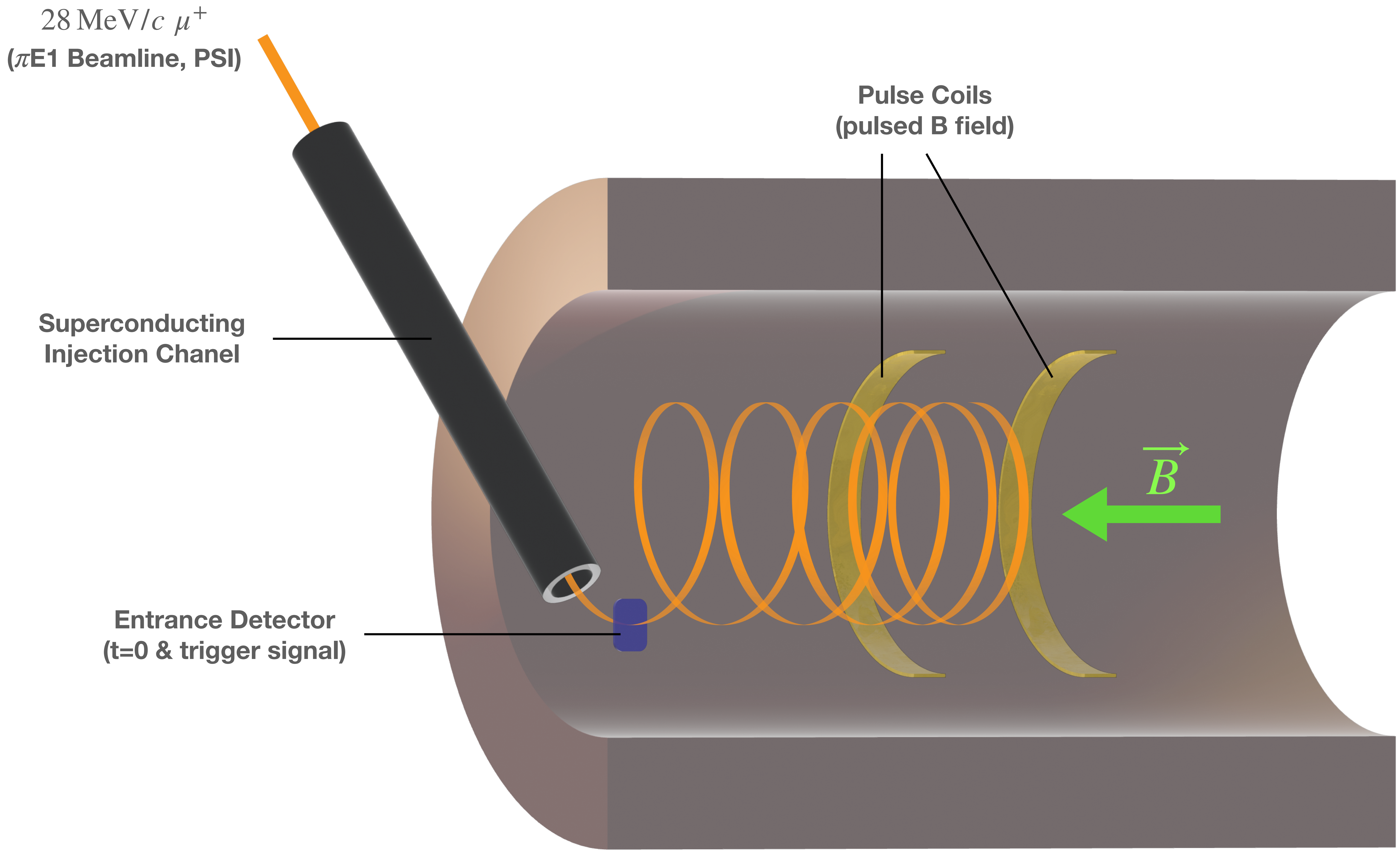

muEDM Experiment at PSI

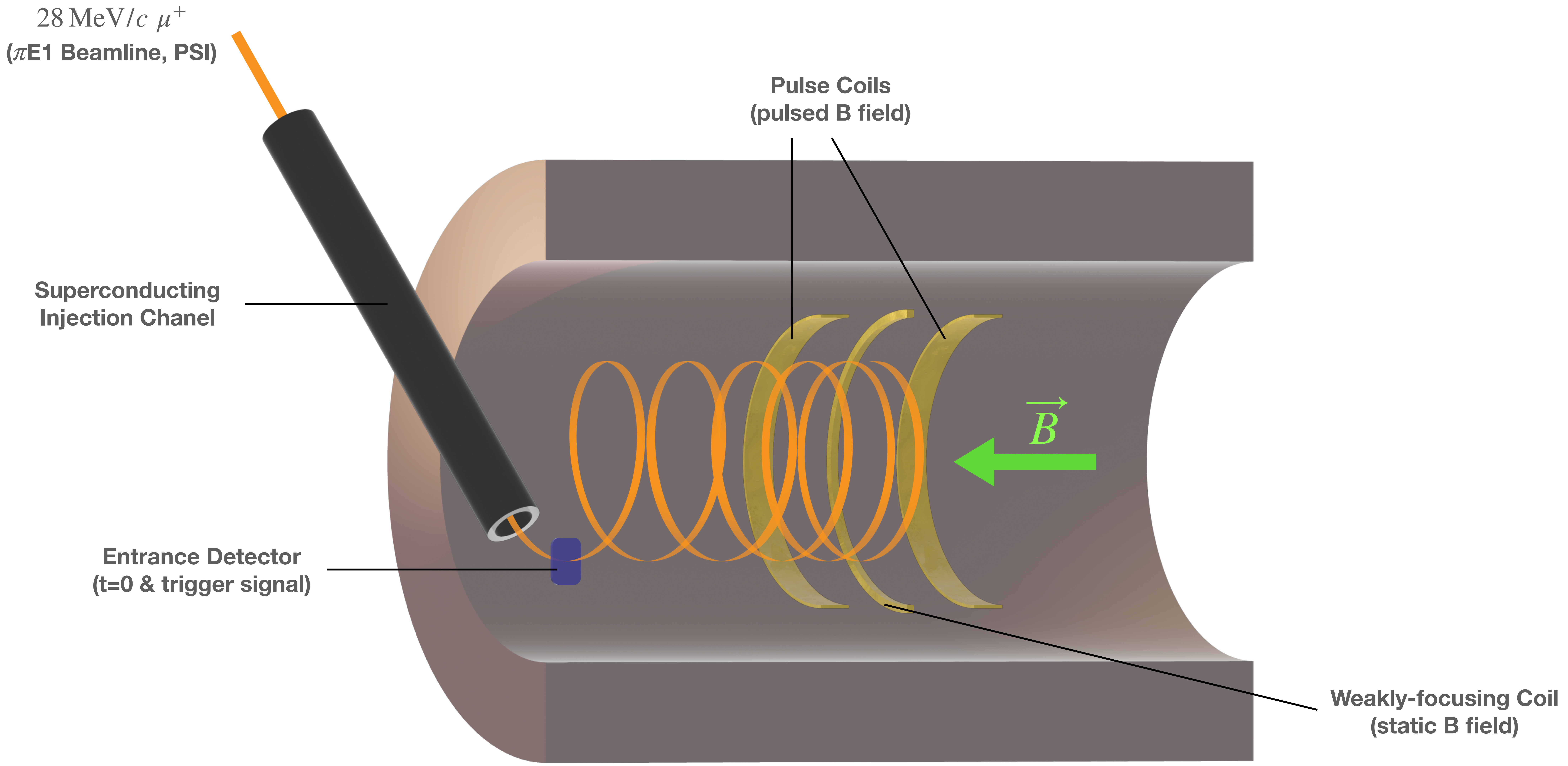

muEDM Experiment at PSI

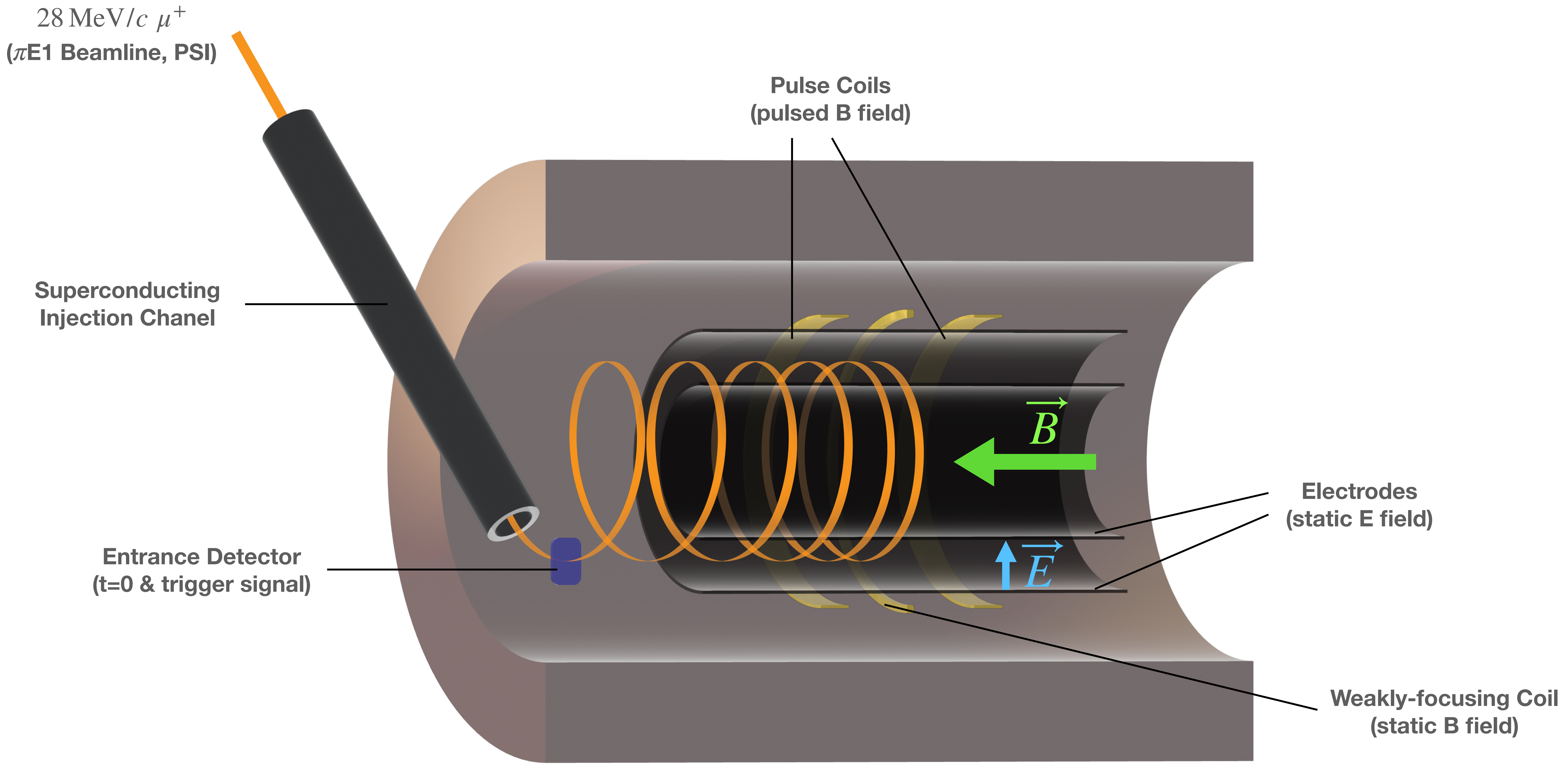

muEDM Experiment at PSI

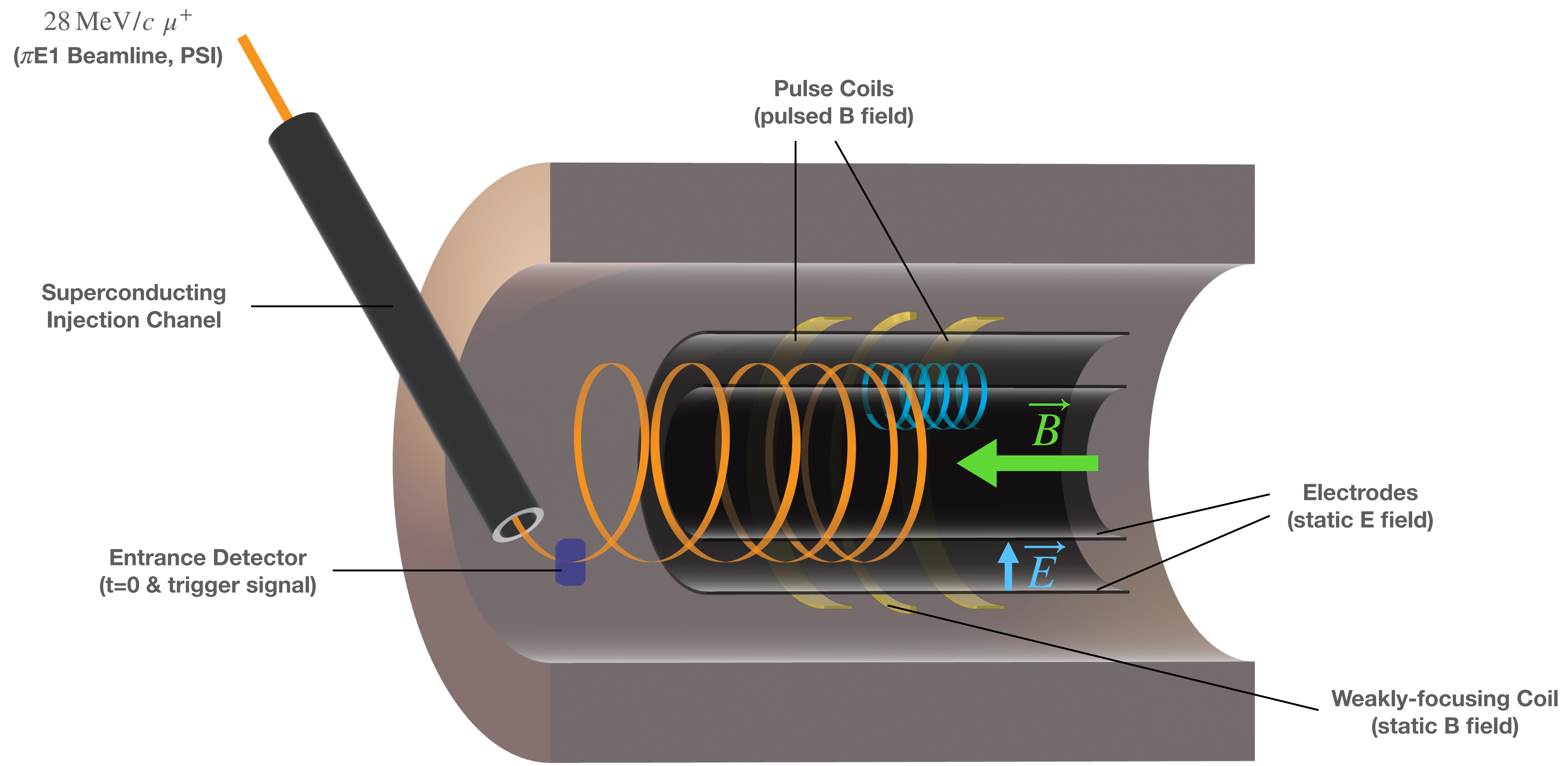

muEDM Experiment at PSI

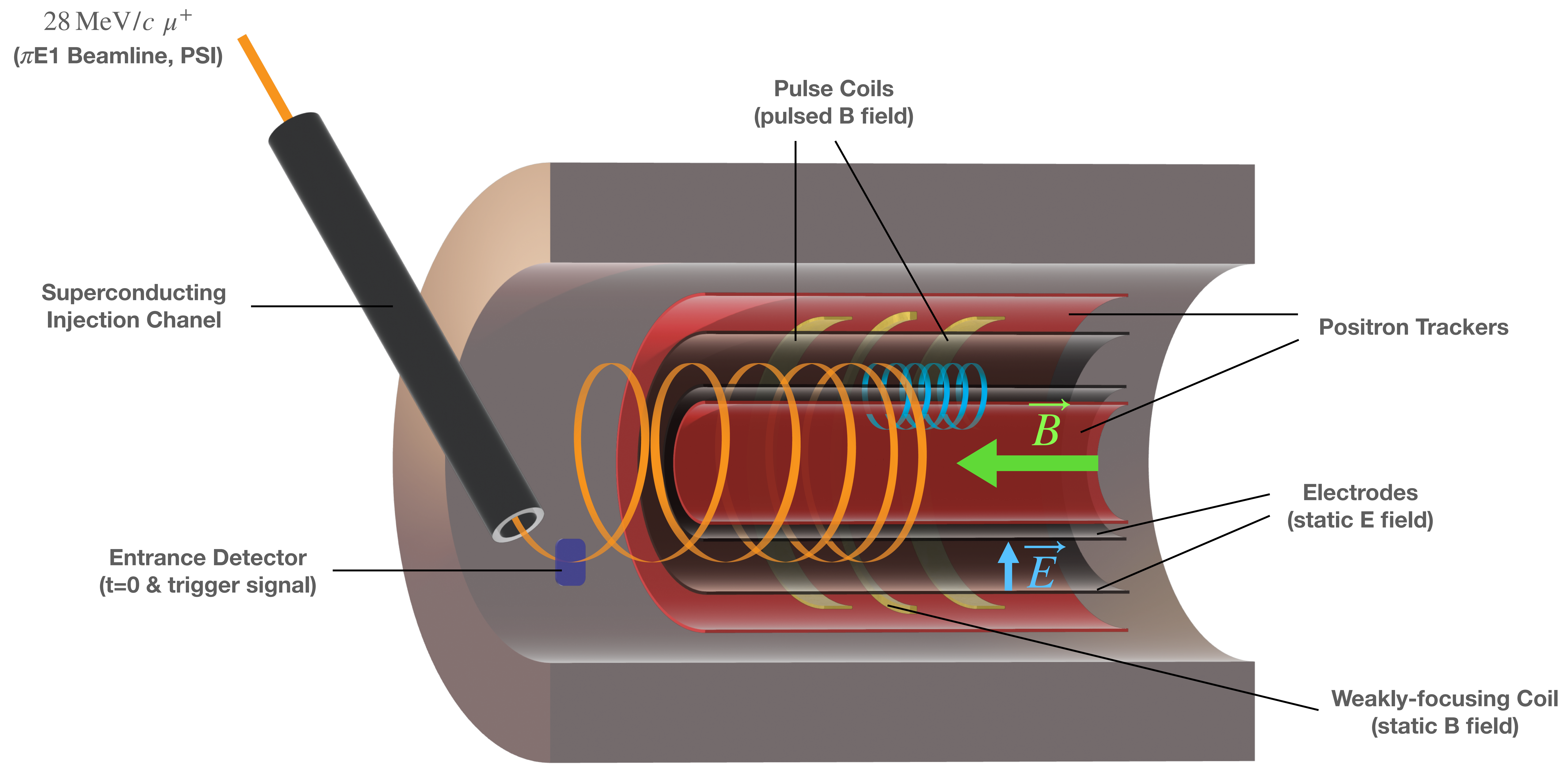

Magnetic Kick Specifications

- **Objective:** stable orbit by kicking longitudinal momentum into the transverse plane as muon enters weakly-focusing storage region.

- **Technical Problem:** High amplitude, short duration pulsed magnetic field must be rapidly triggered.

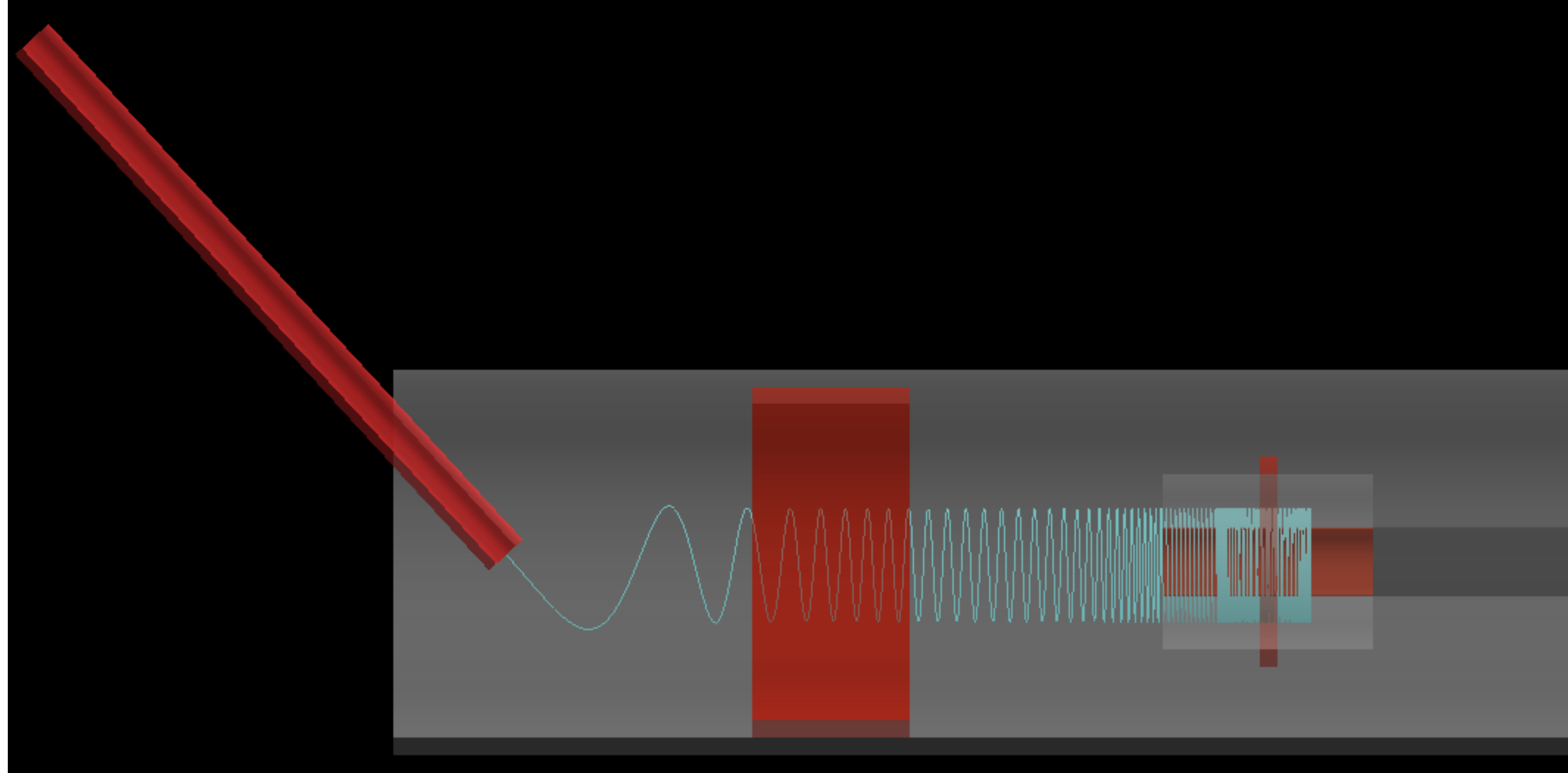

G4 Beamline simulations (R. Chakraborty, PSI) indicate a transit time of **105ns** from **injection** to the **centre** of the 1m solenoid.

Magnetic Kick Specifications

- **Objective:** stable orbit by kicking longitudinal momentum into the transverse plane as muon enters weakly-focusing storage region.

- **Technical Problem:** High amplitude, short duration pulsed magnetic field must be rapidly triggered.

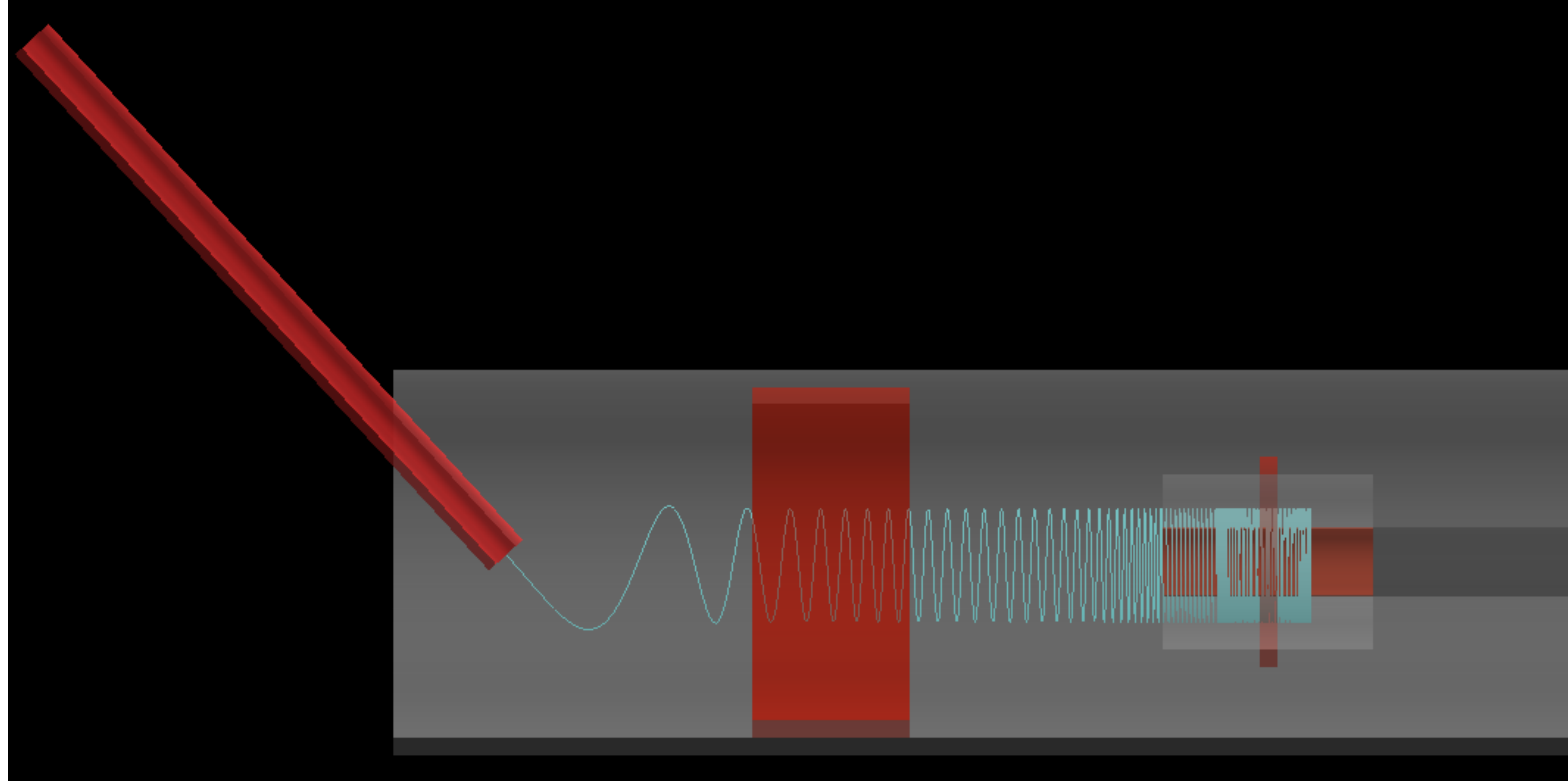

G4 Beamline simulations (R. Chakraborty, PSI) indicate a transit time of **105ns** from **injection** to the **centre** of the 1m solenoid.

Kick Magnitude

- The longitudinal momentum of the muon as it approaches the storage region ($< 1\,\mathrm{MeV}/c$) is much lower than its initial value at injection ($\sim 20\,\mathrm{MeV}/c$).

Kick Magnitude

- The longitudinal momentum of the muon as it approaches the storage region ($< 1\,\mathrm{MeV}/c$) is much lower than its initial value at injection ($\sim 20\,\mathrm{MeV}/c$).

The change in transverse momentum due to the radial component of the **fringe fields of the solenoid** (length 1m) can be approximated from the change in the field strength along the central axis:

$$\frac{\mathrm{d}p_\phi}{\mathrm{d}z} = -\frac{e\rho}{2}\frac{\mathrm{d}B}{\mathrm{d}z}$$

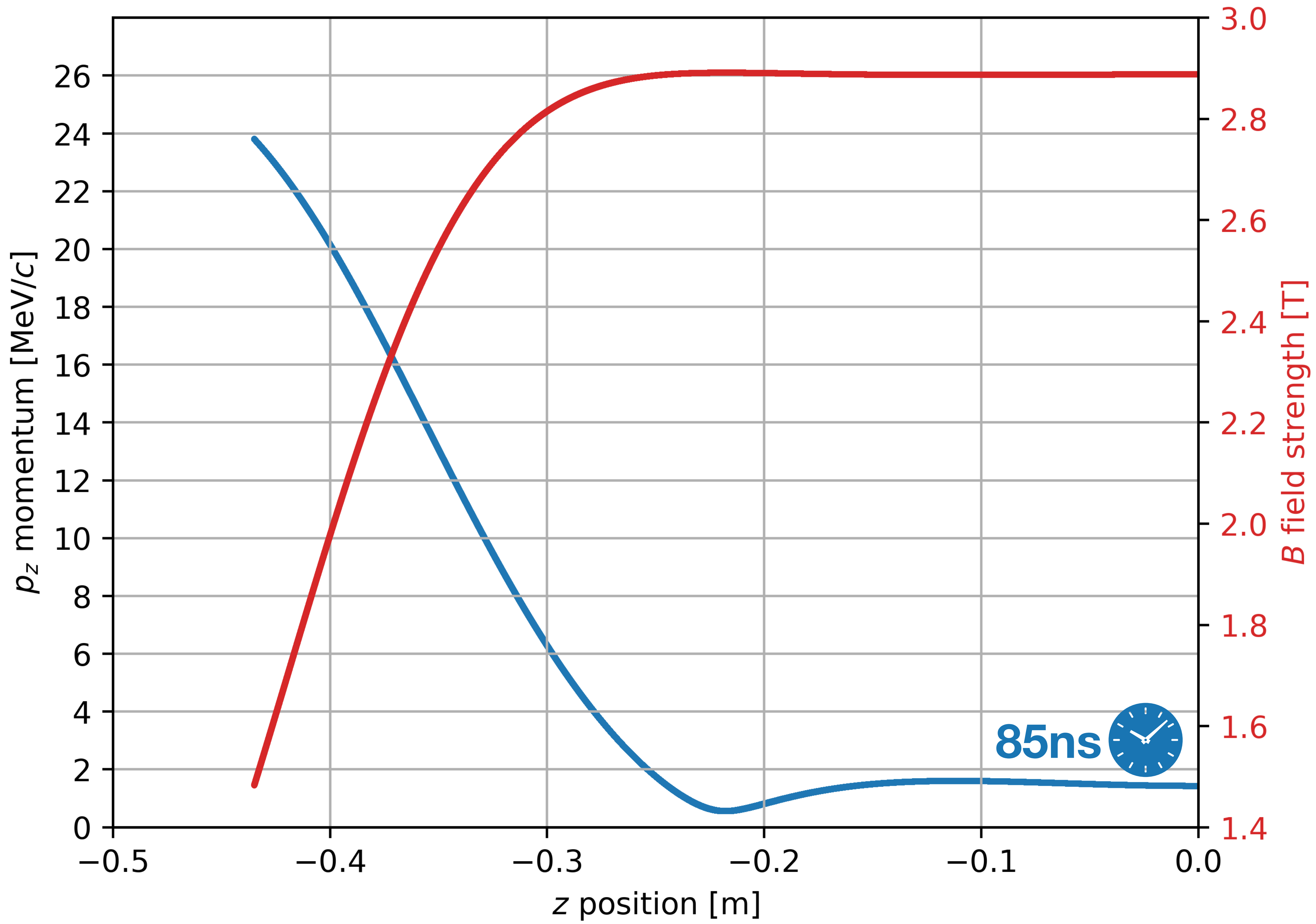

Kick Magnitude

- The longitudinal momentum of the muon as it approaches the storage region ($< 1\,\mathrm{MeV}/c$) is much lower than its initial value at injection ($\sim 20\,\mathrm{MeV}/c$).

The change in transverse momentum due to the radial component of the **fringe fields of the solenoid** (length 1m) can be approximated from the change in the field strength along the central axis:

$$\frac{\mathrm{d}p_\phi}{\mathrm{d}z} = -\frac{e\rho}{2}\frac{\mathrm{d}B}{\mathrm{d}z}$$

The radial component of the pulsed field is responsible for **kicking the remaining longitudinal momentum:**

$$\dot{\vec{p}}(t) = \frac{e}{\gamma m}\vec{p} \times \overrightarrow{B}_{\mathrm{pulse}}(t)$$

$$\implies \dot{p}_z(t) = \frac{e}{\gamma m} p_\phi \overrightarrow{B}_{\mathrm{pulse}}(t) \cdot \hat{\rho}$$

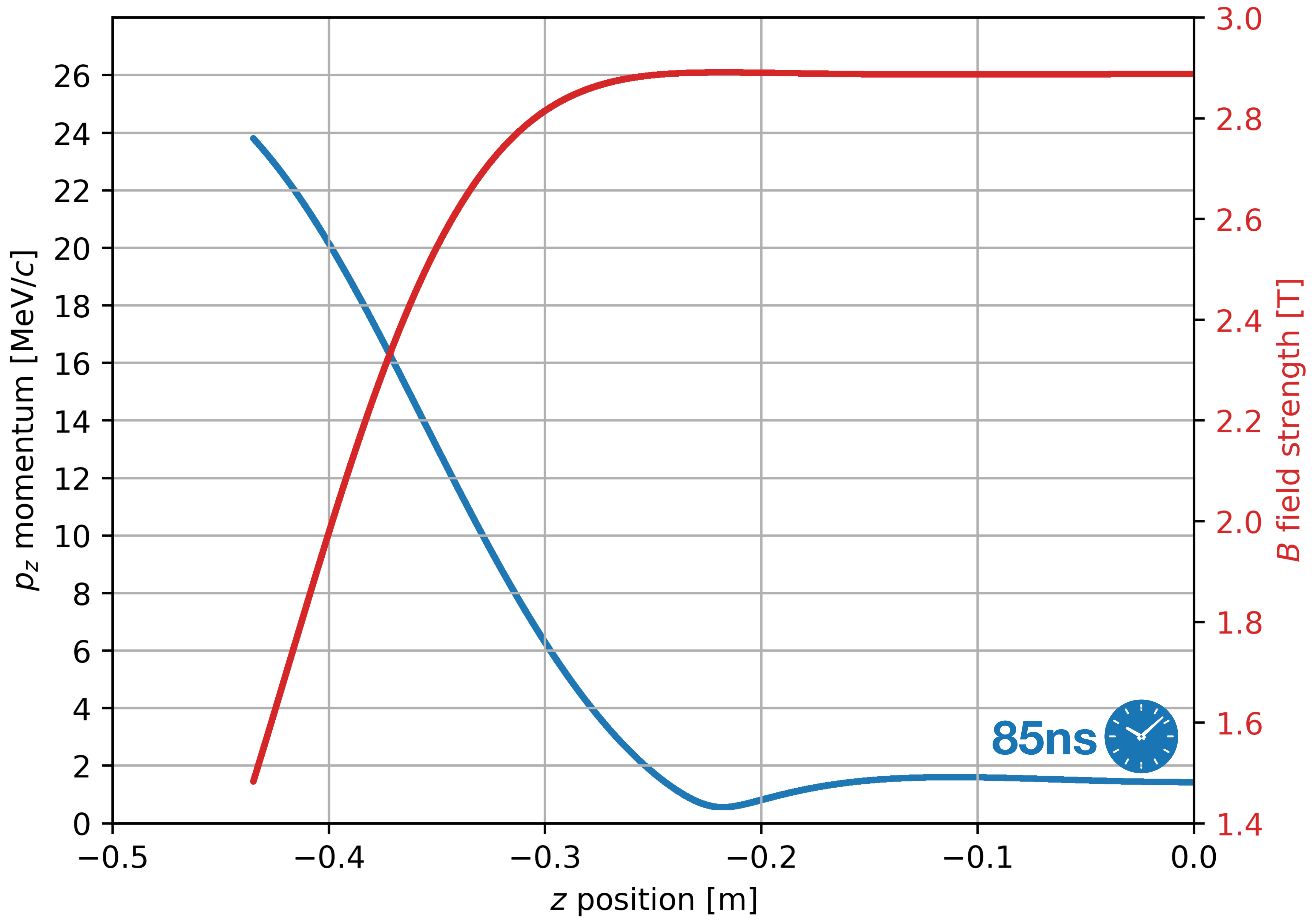

Kick Magnitude

- The longitudinal momentum of the muon as it approaches the storage region ($< 1\,\mathrm{MeV}/c$) is much lower than its initial value at injection ($\sim 20\,\mathrm{MeV}/c$).

The change in transverse momentum due to the radial component of the **fringe fields of the solenoid** (length 1m) can be approximated from the change in the field strength along the central axis:

$$\frac{\mathrm{d}p_\phi}{\mathrm{d}z} = -\frac{e\rho}{2}\frac{\mathrm{d}B}{\mathrm{d}z}$$

The radial component of the pulsed field is responsible for **kicking the remaining longitudinal momentum:**

$$\dot{\vec{p}}(t) = \frac{e}{\gamma m}\vec{p} \times \vec{B}_{\mathrm{pulse}}(t)$$

$$\implies \dot{p}_z(t) = \frac{e}{\gamma m} p_\phi \vec{B}_{\mathrm{pulse}}(t) \cdot \hat{\rho}$$

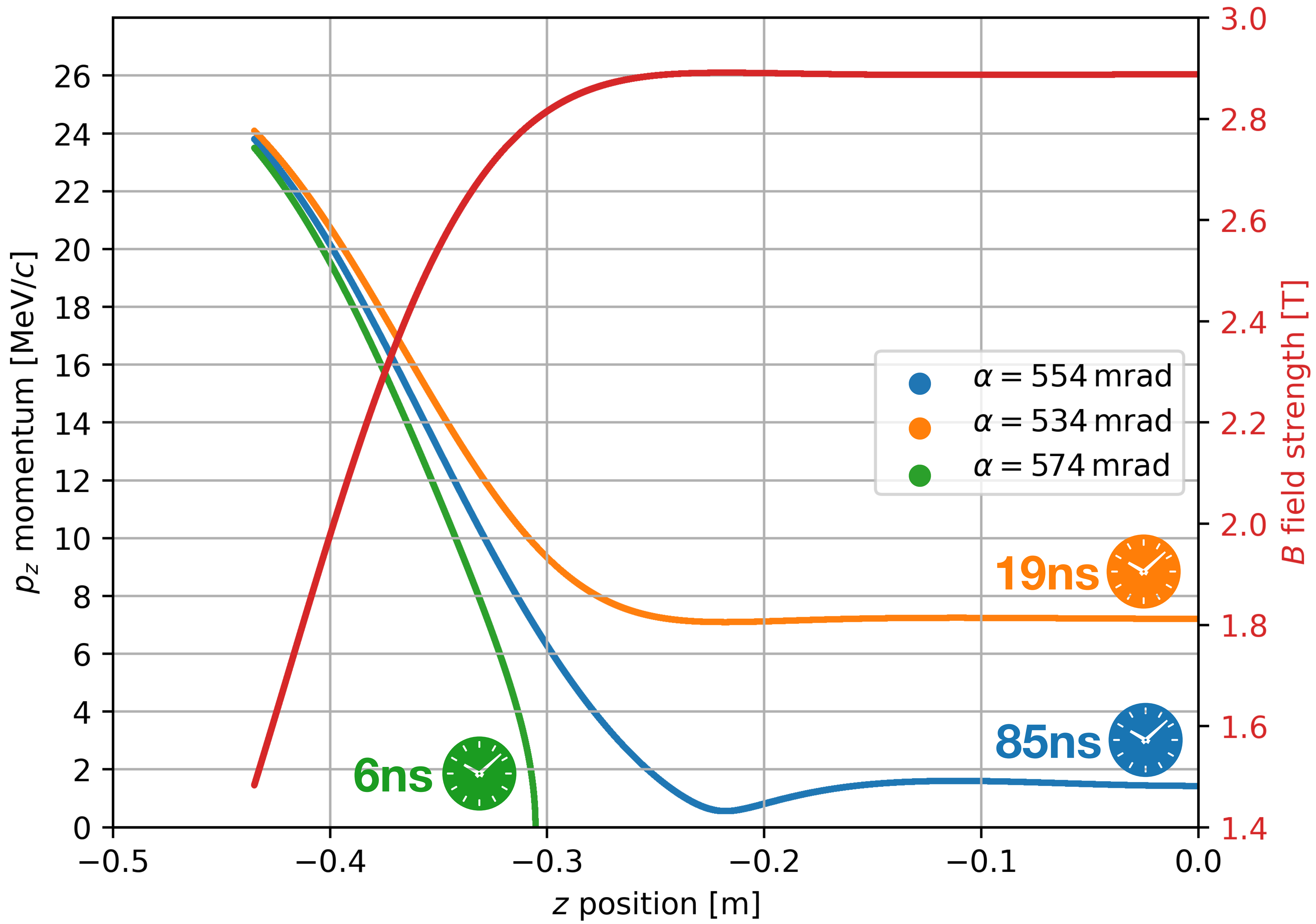

Injection calculation for illustration only - estimated using coarse field map of 3T solenoid and first order approximation for evolution of transverse momentum as described. Optimised injections parameters are the subject of G4Beamline simulations by R. Chakraborty.

Pulse Coils

- Anti-Helmholtz configuration to supply strong radial component of the pulsed magnetic field.
- To kick the longitudinal momentum will require a total current $\sim 100\,\mathrm{A}$ through each coil for a full width $\sim 50\,\mathrm{ns}$.

Radial Projection of B Field

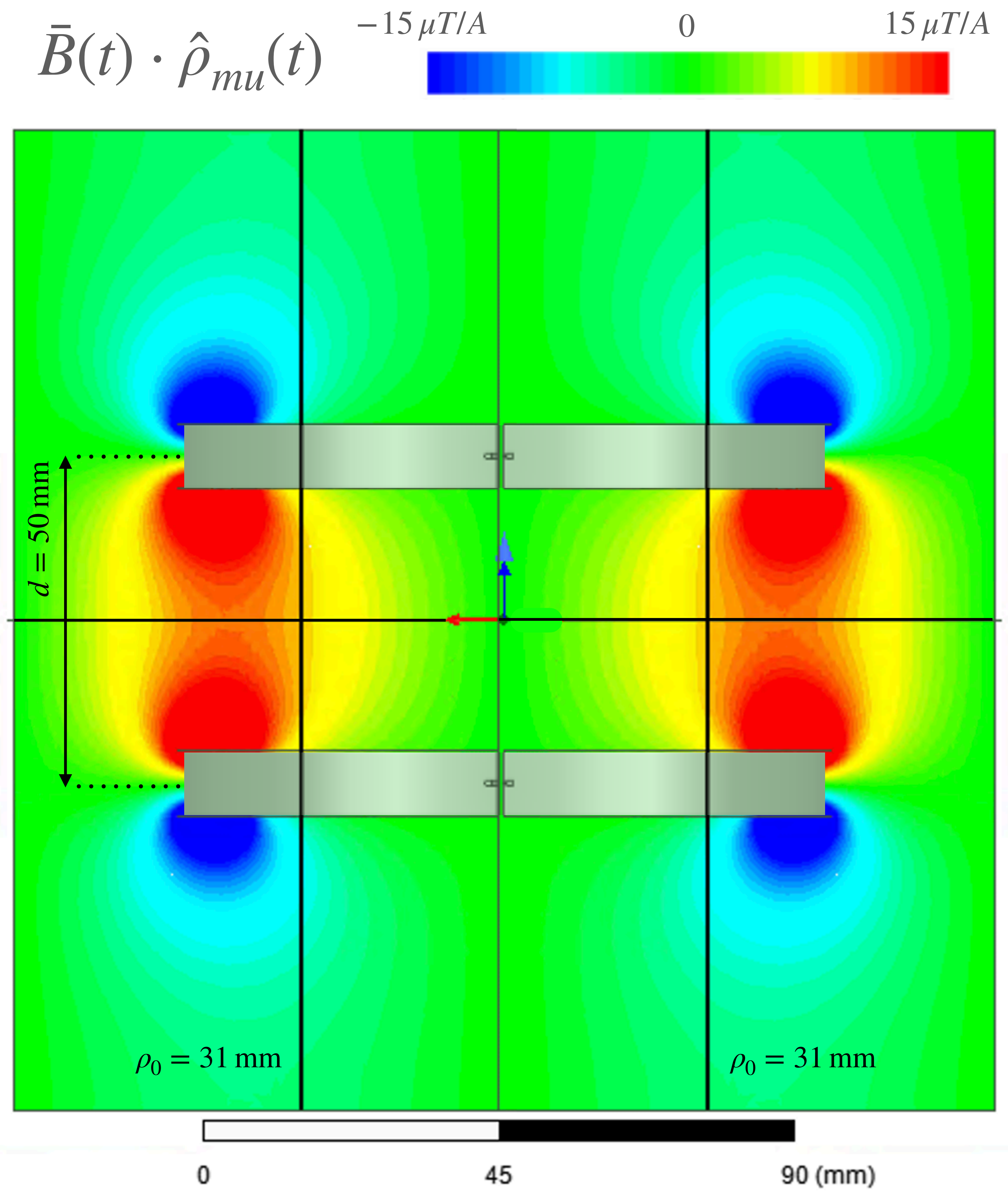

$\hat{\rho}_{mu}(t)$ = radial coordinate of muon path in cylindrical coordinate system. The B field radial projection thus kicks the longitudinal momentum.

Pulse Coil Design Optimisation

- Inductance must be minimised to drive high amplitude current pulse with fast rise/fall time and suppress after-pulse oscillations.

Coil prototypes: Cu, $\phi 100\,\mathrm{mm}$, $10 \times 10\,\mathrm{mm}^2$

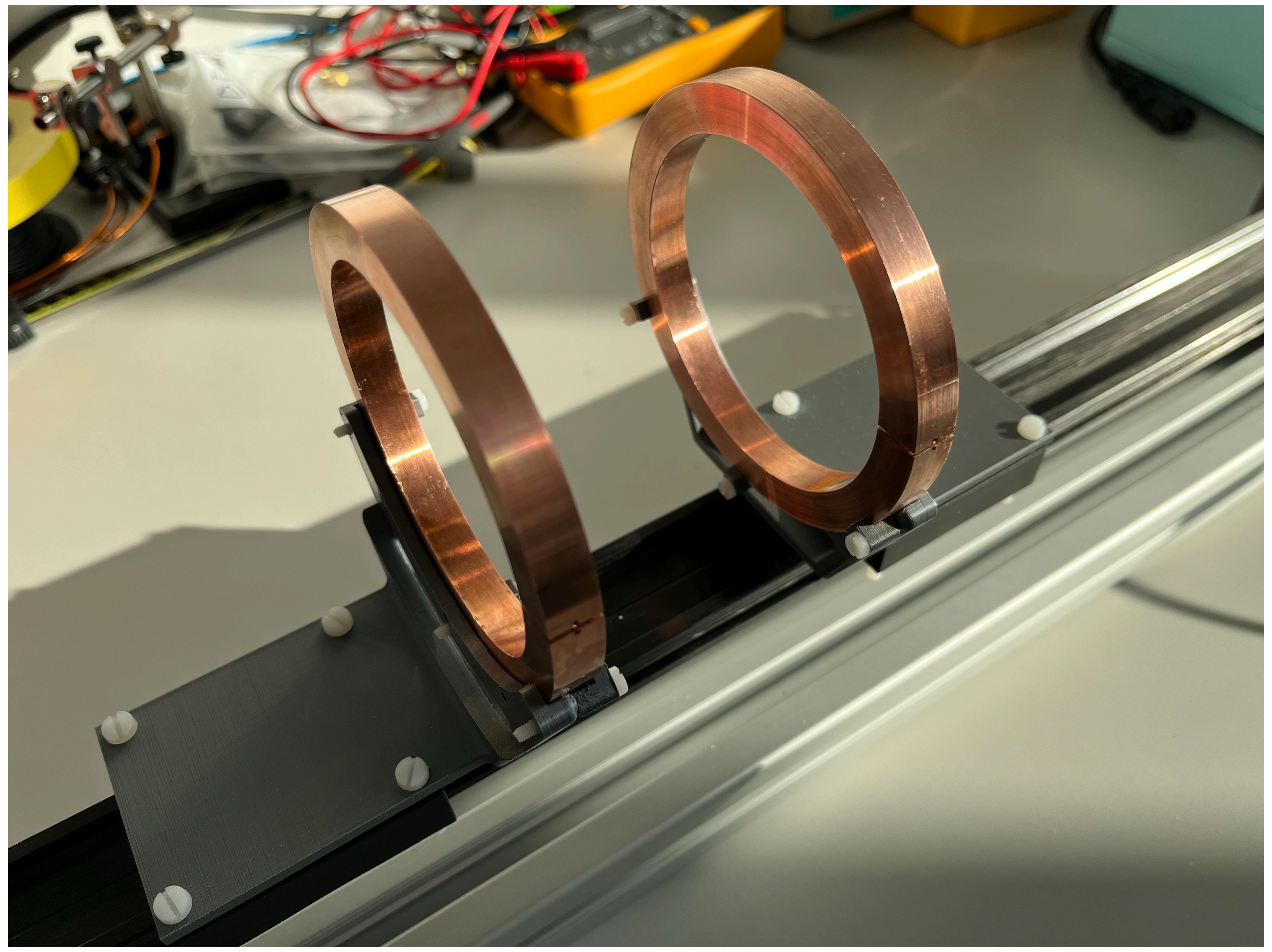

After-pulse oscillations

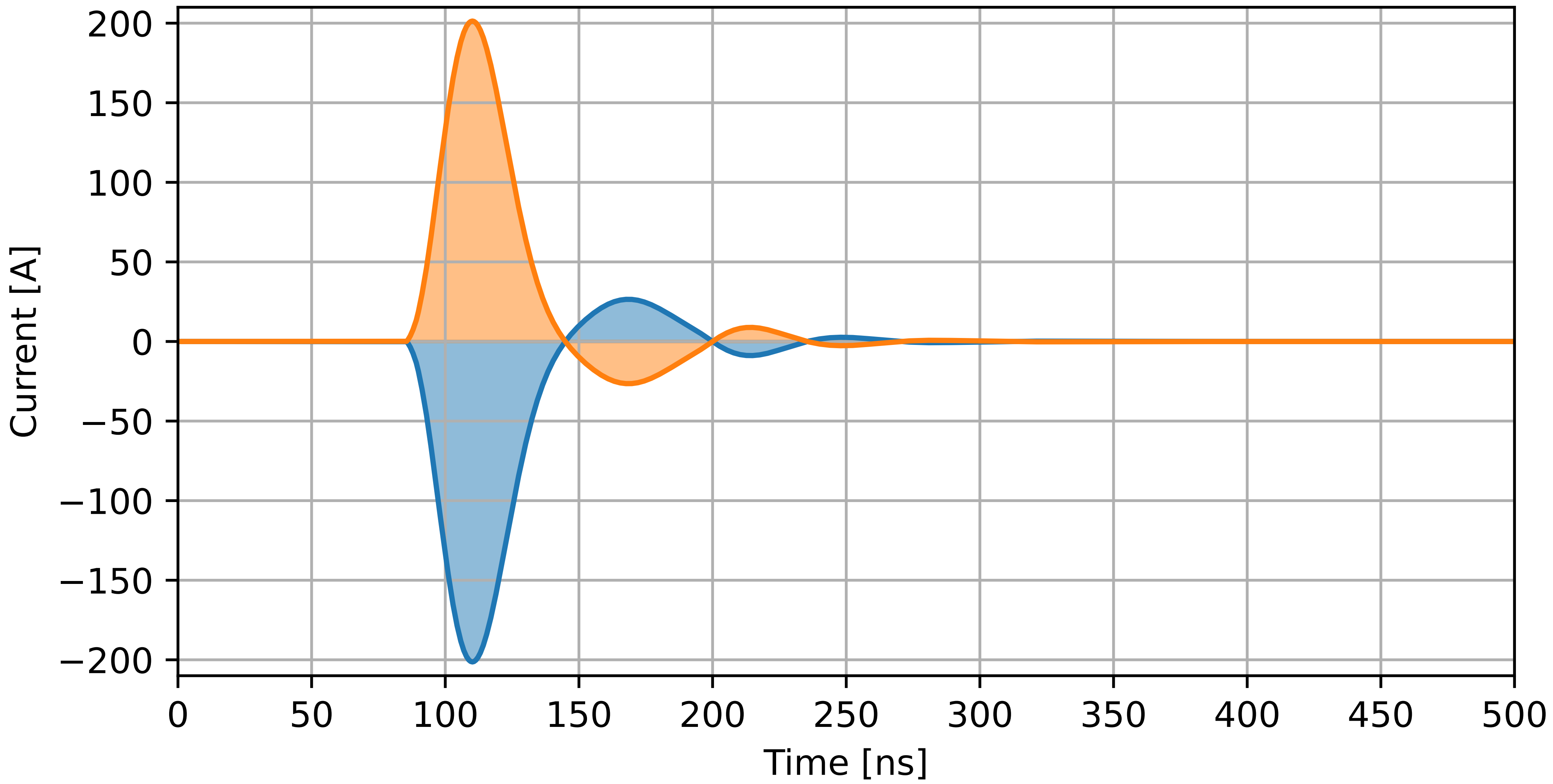

Pulse Coil Design Optimisation

- Inductance must be minimised to drive high amplitude current pulse with fast rise/fall time and suppress after-pulse oscillations.

- Self inductance of each coil:
  - Measured: $L = 121 \pm 1\,\mathrm{nH}$
  - Wire-loop Calculation: $L = 129\,\mathrm{nH}$
  - Ansys FEM: $L = 139\,\mathrm{nH}$

Coil prototypes: Cu, $\phi 100\,\mathrm{mm}$, $10 \times 10\,\mathrm{mm}^2$

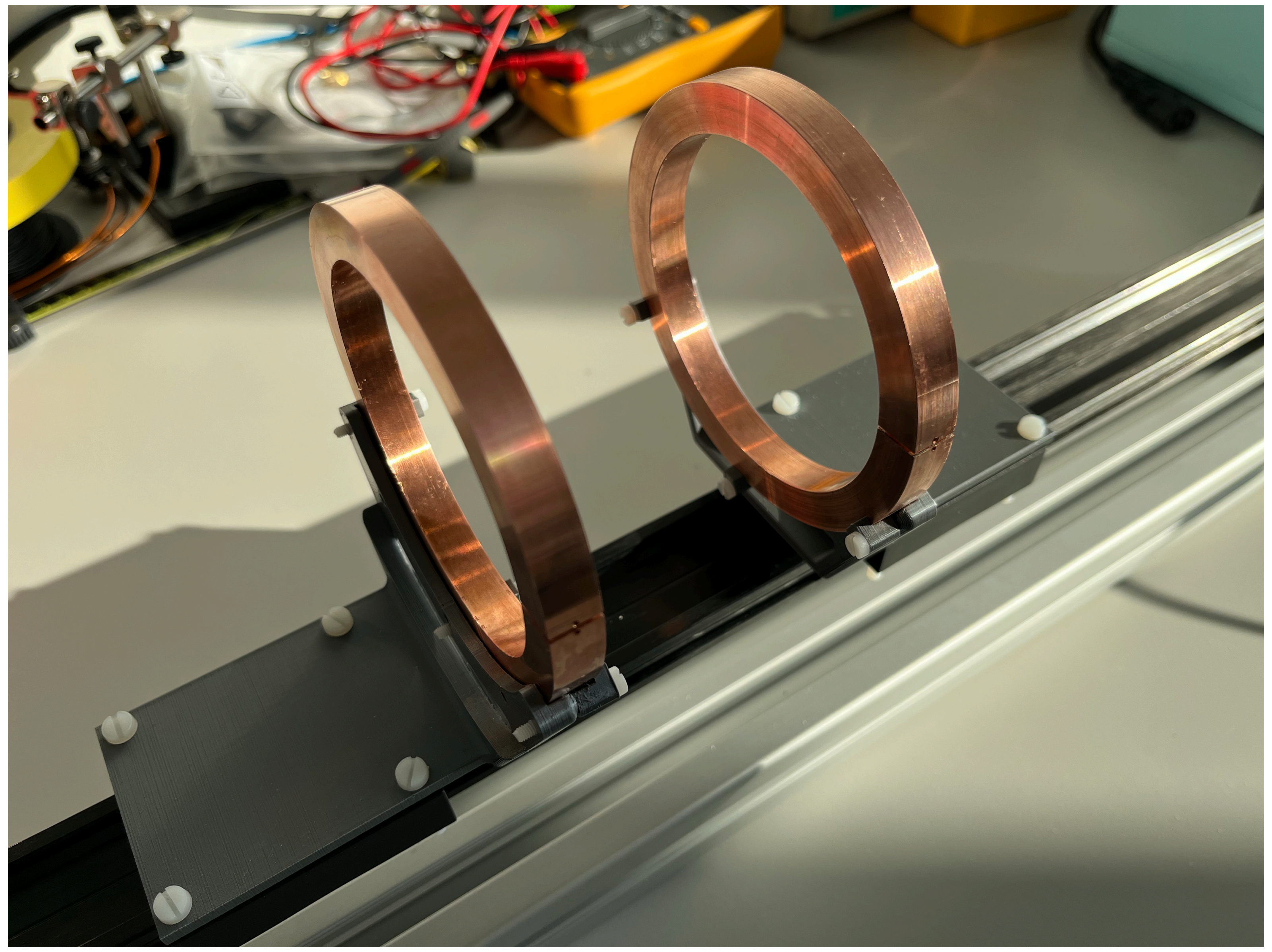

After-pulse oscillations

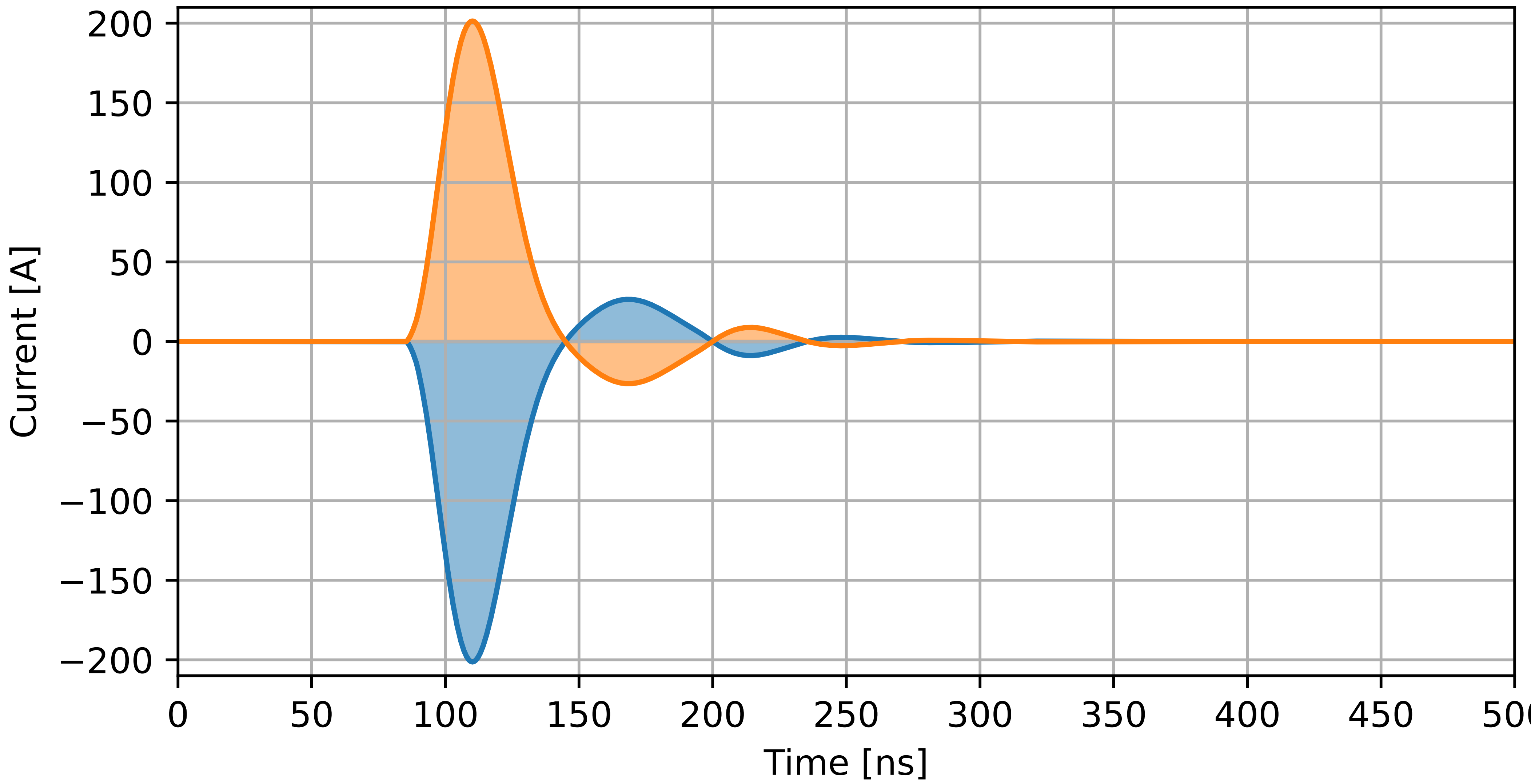

Pulse Coil Design Optimisation

- Inductance must be minimised to drive high amplitude current pulse with fast rise/fall time and suppress after-pulse oscillations.

- Self inductance of each coil:
  - Measured: $L = 121 \pm 1\,\mathrm{nH}$
  - Wire-loop Calculation: $L = 129\,\mathrm{nH}$
  - Ansys FEM: $L = 139\,\mathrm{nH}$

- Coil geometry optimisation also based on
  - Material budget in e^+ acceptance
  - Low effective resistance at high frequencies

Coil prototypes: Cu, $\phi 100\,\mathrm{mm}$, $10 \times 10\,\mathrm{mm}^2$

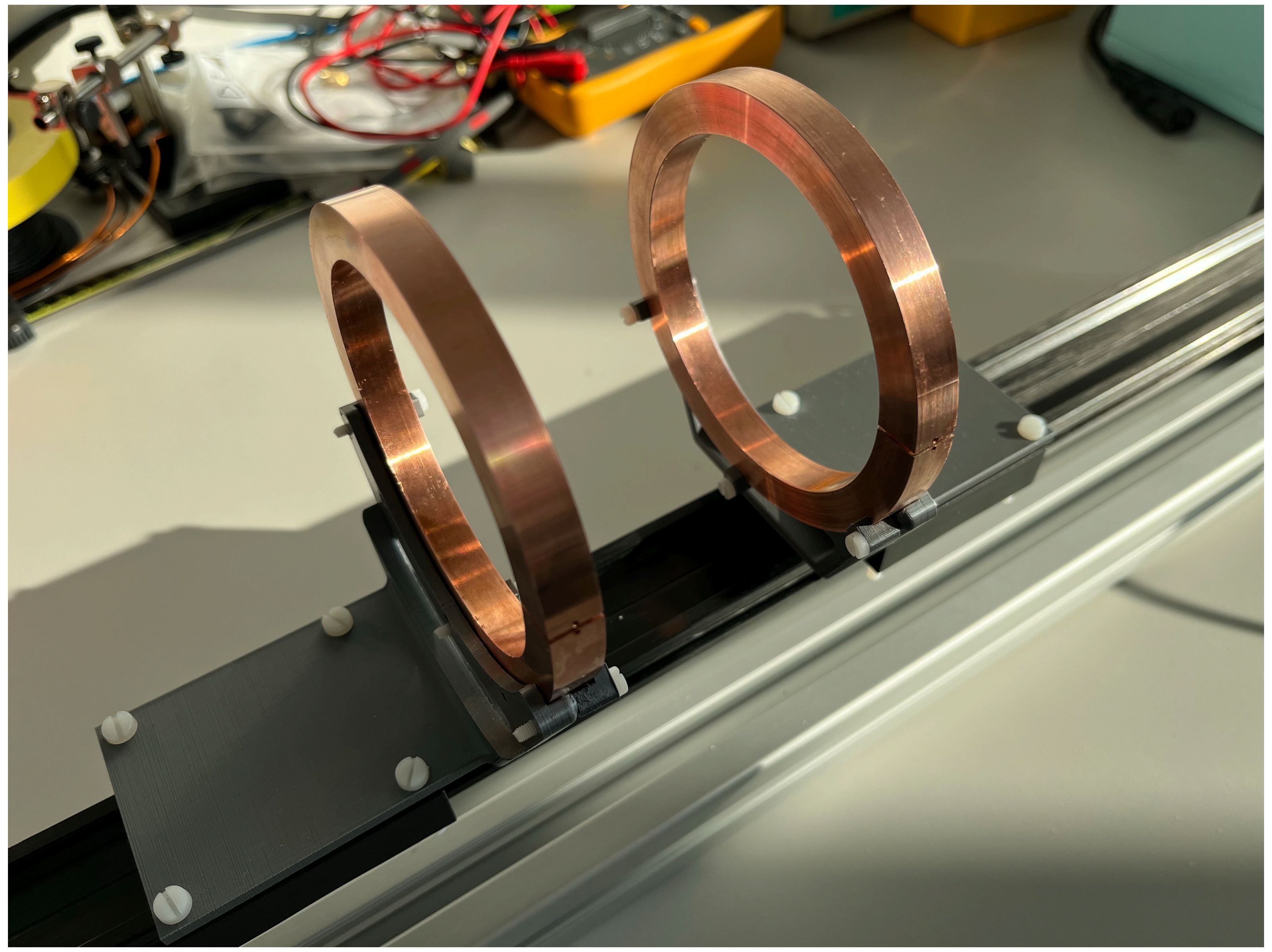

After-pulse oscillations

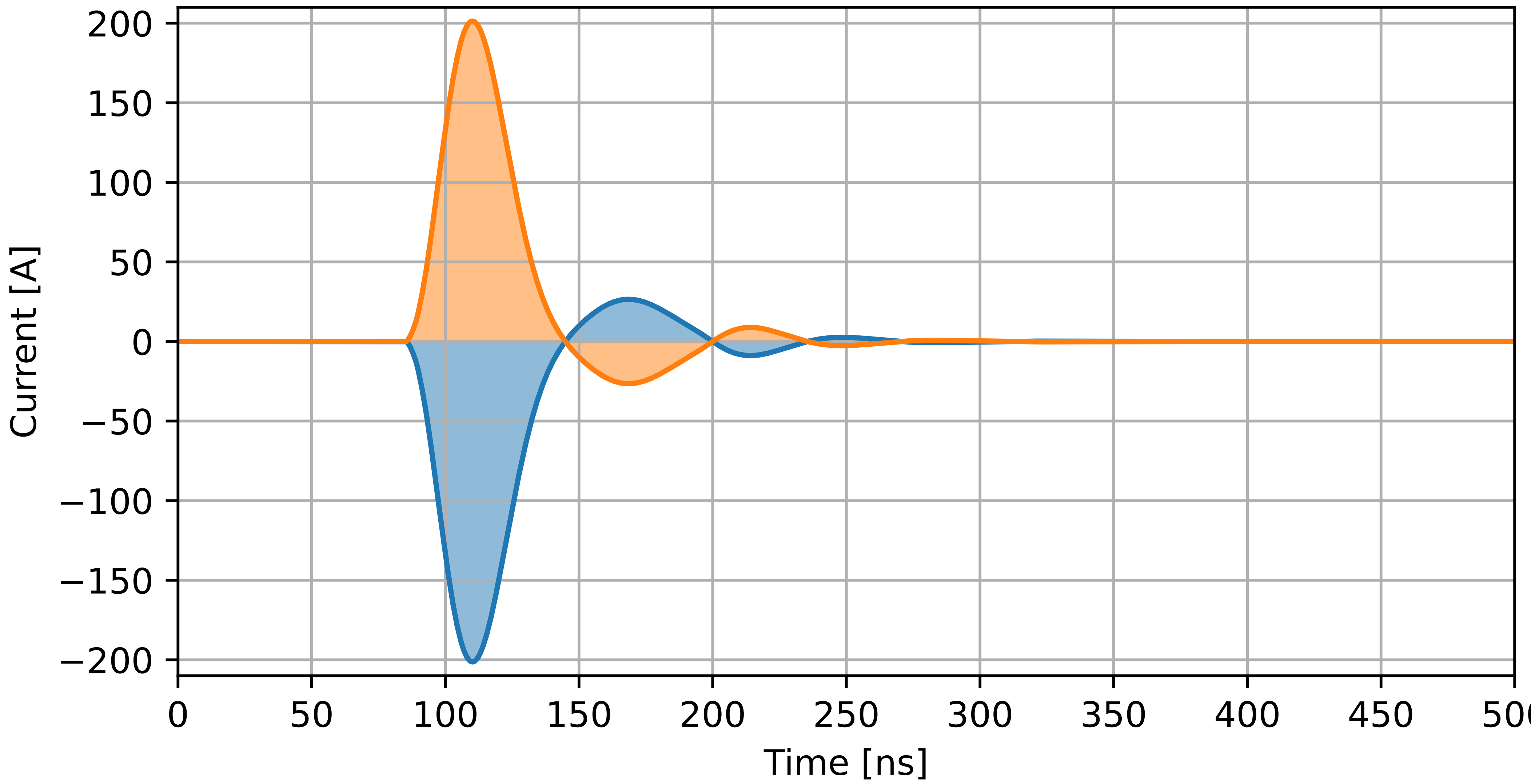

Eddy Currents & Magnetic Field Damping

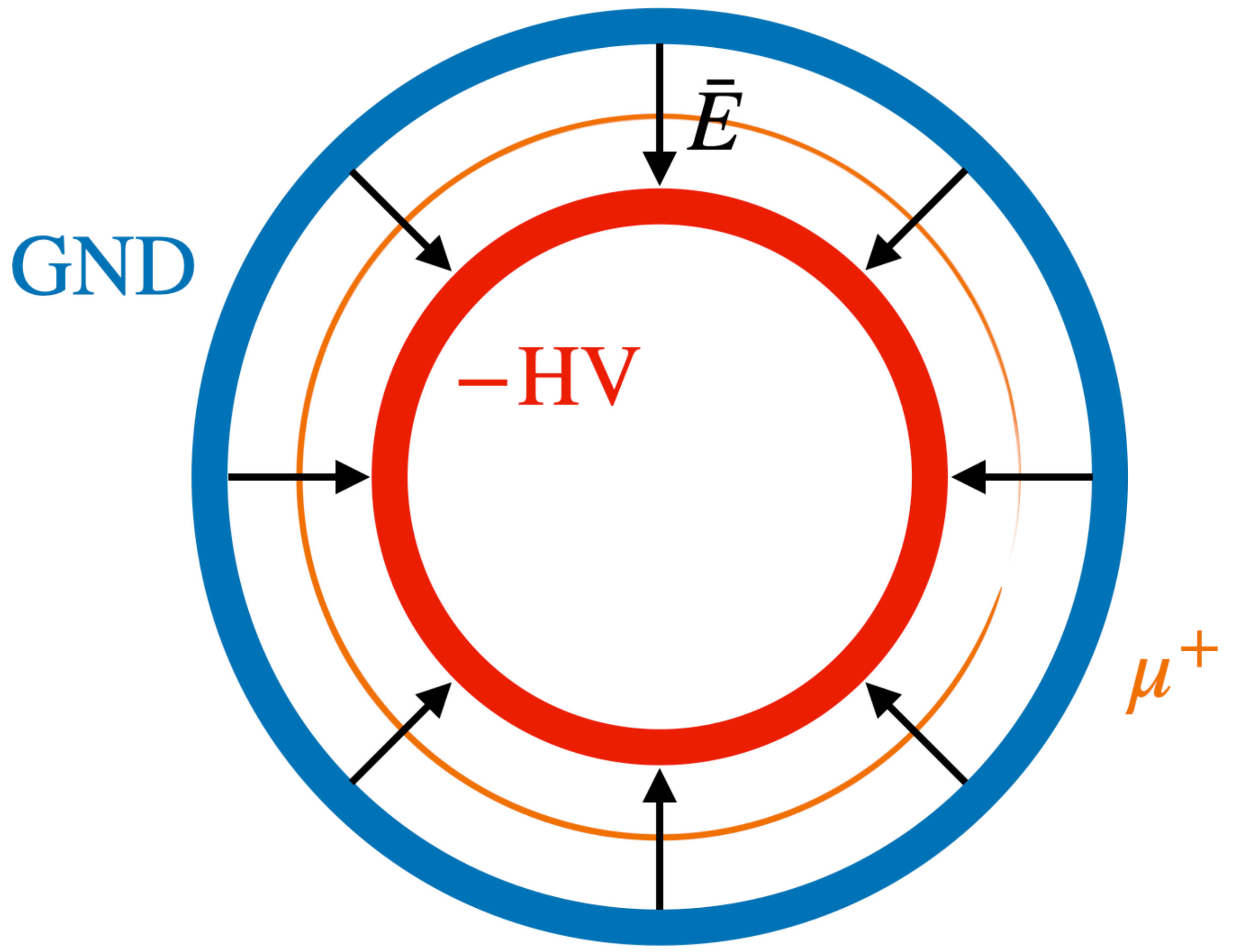

- **Problem:** The magnetic field seen by the muon will be suppressed by the induced eddy currents.
- **Solution:** To achieve the field strength necessary to trap the muons in the storage region, we must:
  - Increase current; or
  - Optimise electrode geometry & material

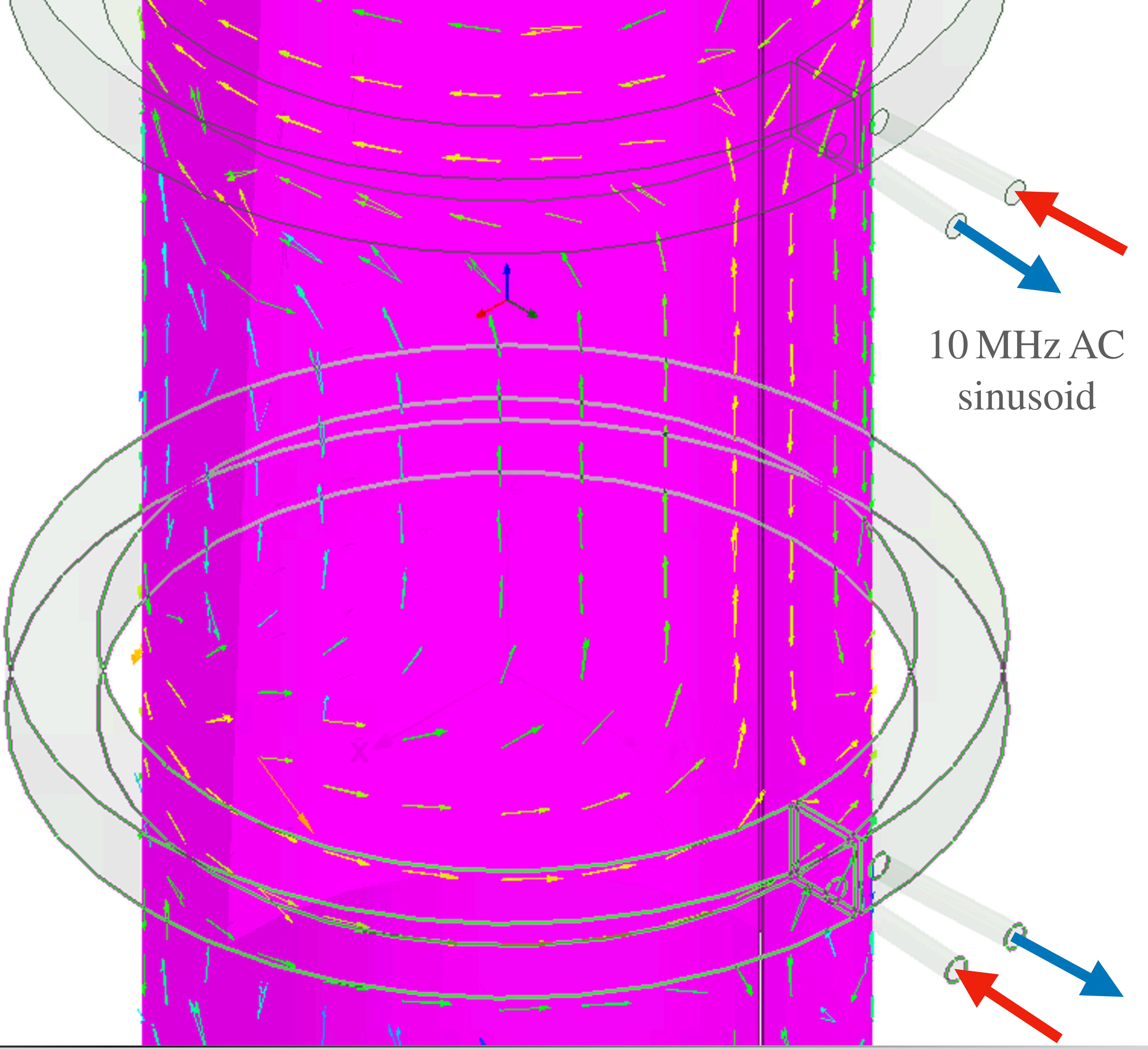

Frozen-spin Electrodes

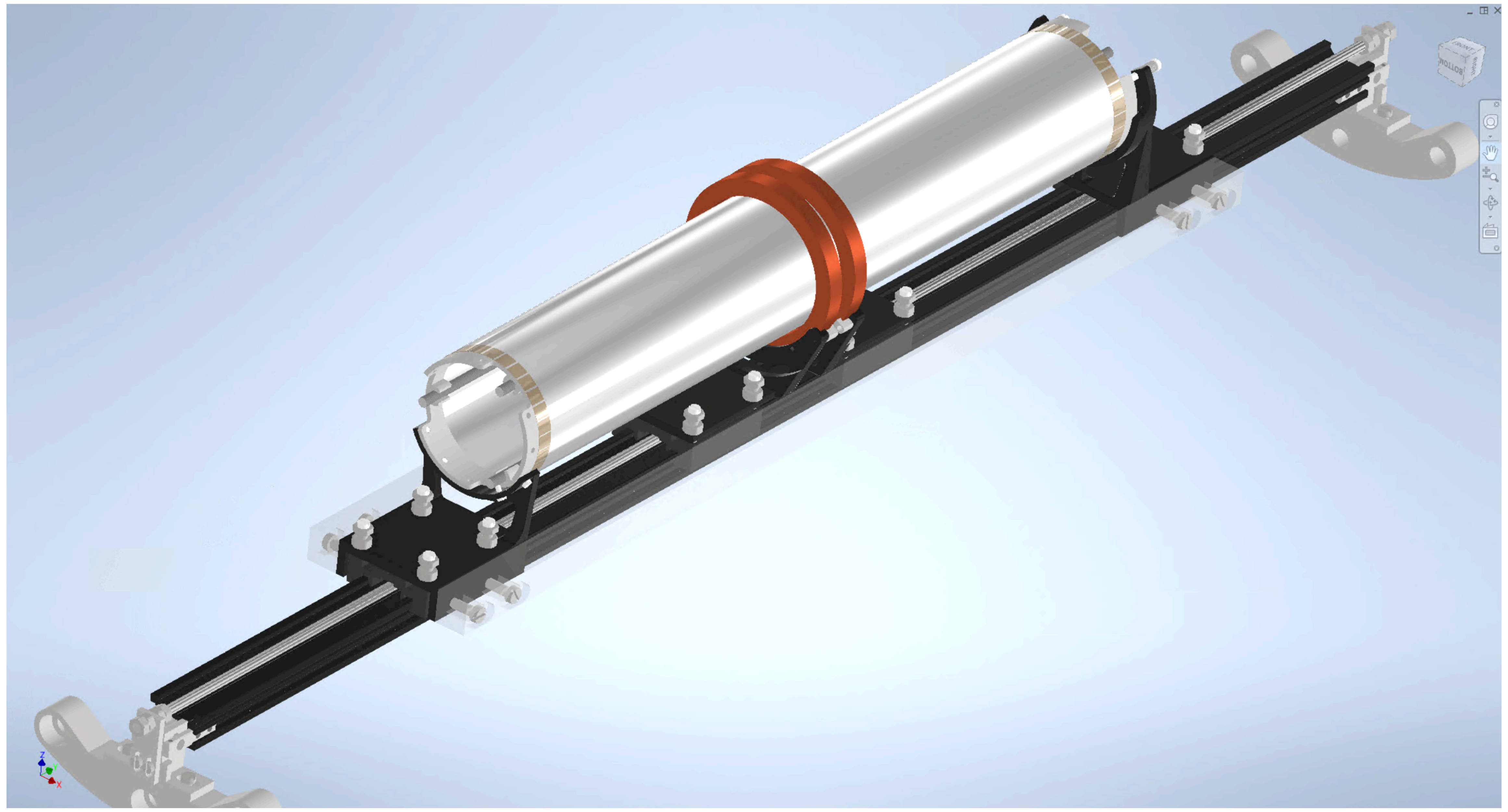

Requirements

- Eddy currents
  - *Low electrical conductivity*
  - *Segmented geometry*
- Precise alignment (limit E_z (axial) - systematic effects)
  - *Material robust as thin foil*
- Material budget
  - *Weak multiple scattering of positrons*

Candidates

- Aluminised polymer (eg. Mylar, Kapton)
  - Advantages: aluminium coating can be very thin, robust
  - Disadvantages: high thermal expansion, high conductivity
- Graphite
  - Advantage: low conductivity
  - Disadvantage: poor mechanical robustness

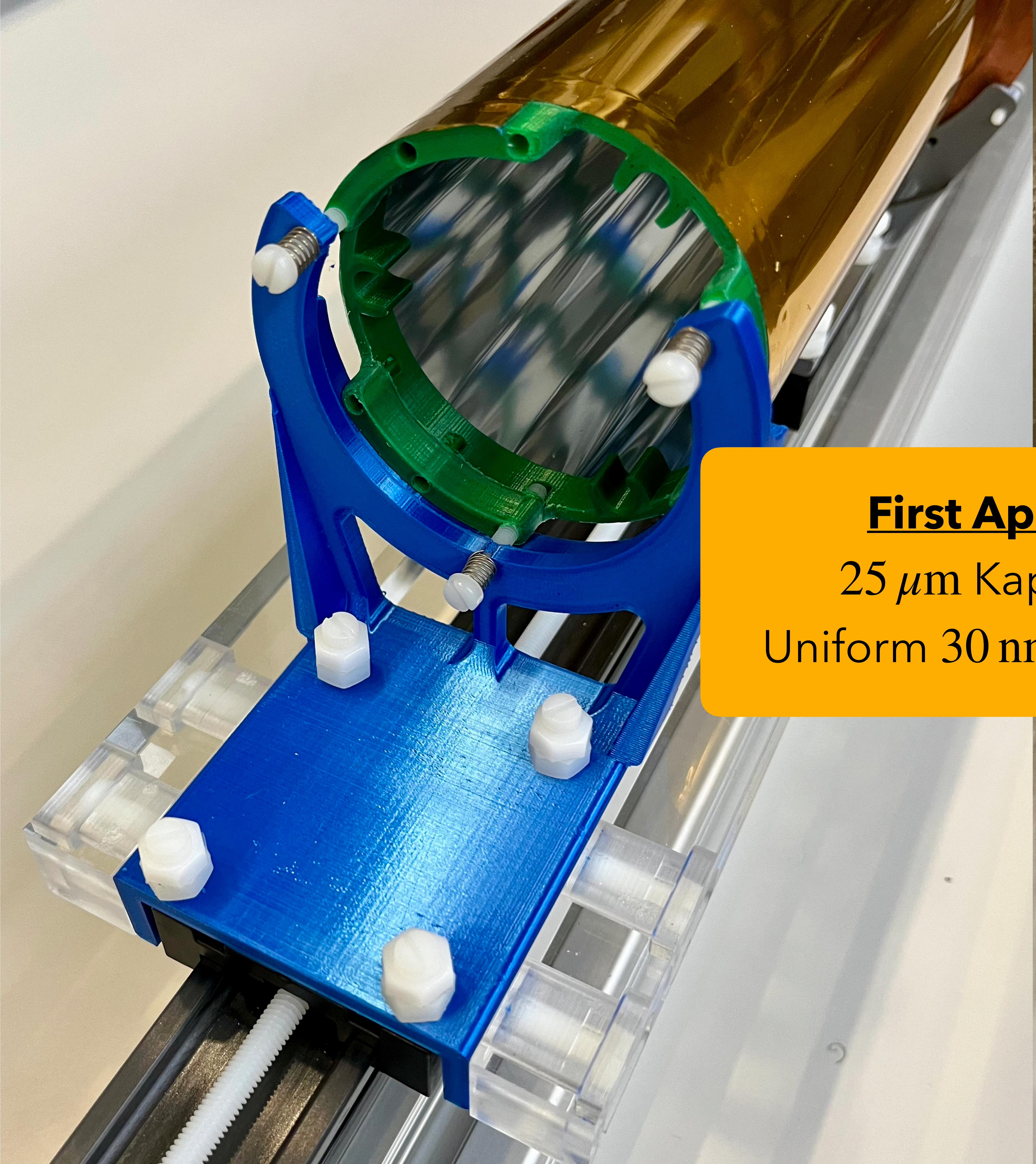

First Approach:

$25\,\mu\mathrm{m}$ Kapton films

Uniform $30\,\mathrm{nm}$ Alu coating

Radial Magnetic Field Measurements

- Measured using a pickup coil ( ) at radius $30.0 \pm 0.5\,\mathrm{mm}$, close to the muon orbit radius.
- Different components added to observe effect, due to induction of eddy currents.

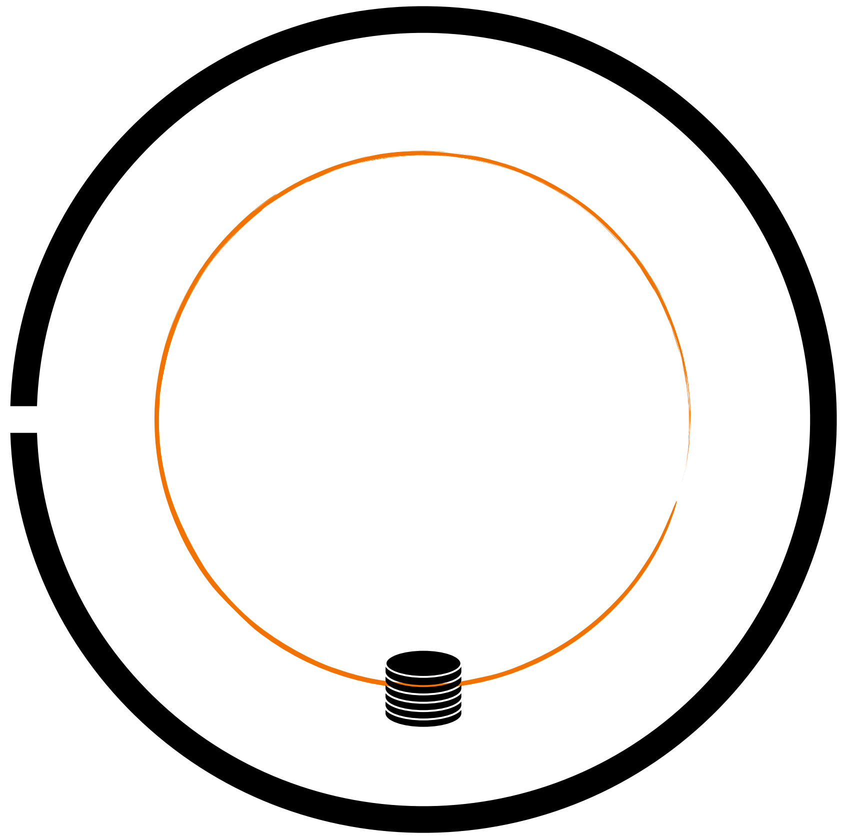

$\mathrm{PulseCoil: Alu, 10 \times 10 mm^2, IR = 40\,mm}$

Field Reference B_{coil}

$$\text{Shielding Factor} = \frac{B_{\mathrm{coil}}}{B}$$

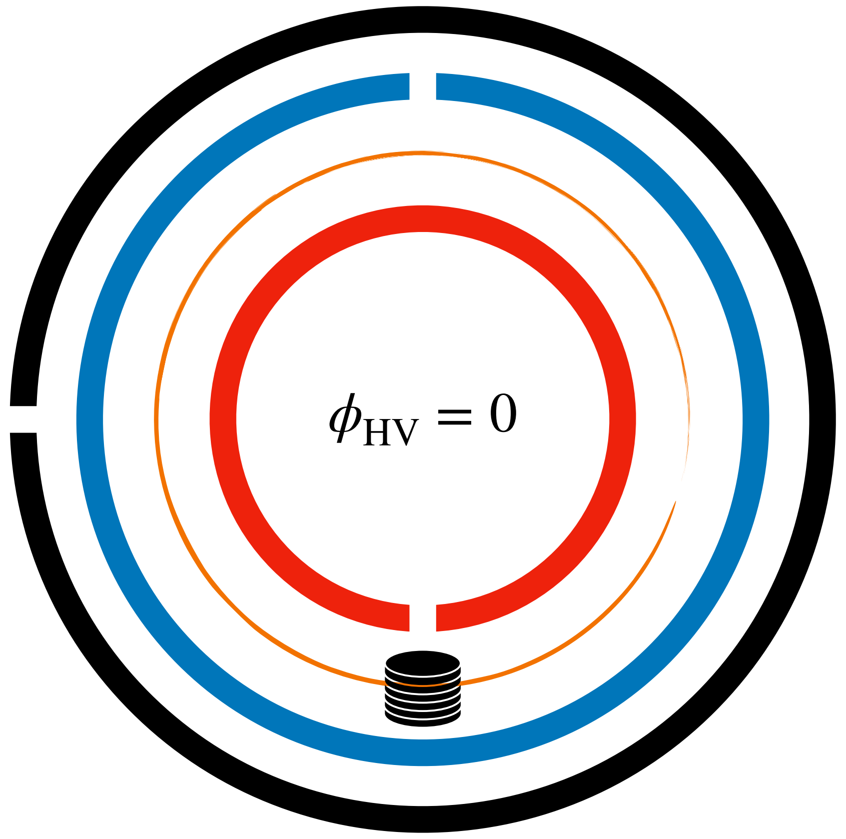

$\mathrm{PulseCoil: Alu, 10 \times 10 mm^2, IR = 40\,mm}$

$\mathrm{GND: Alu/Kapton\ 30\,nm}$

$\mathrm{HV: Alu/Kapton\ 30\,nm}$

Radial Magnetic Field Measurements

- Measured using a pickup coil ( ) at radius $30.0 \pm 0.5\,\mathrm{mm}$, close to the muon orbit radius.
- Different components added to observe effect, due to induction of eddy currents.

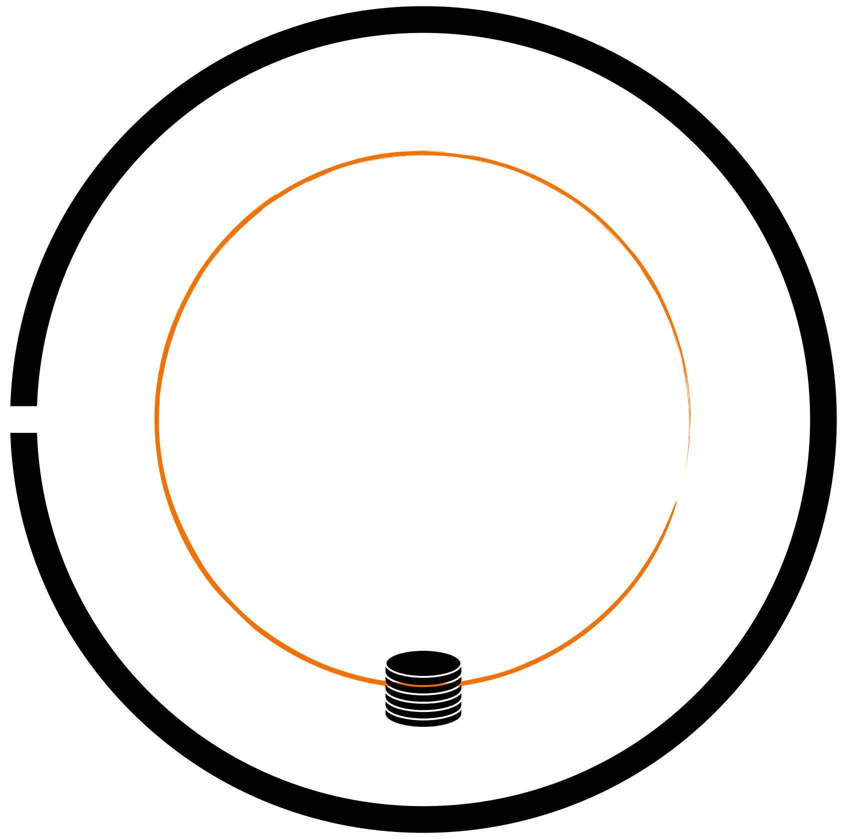

$\mathrm{PulseCoil}: \mathrm{Alu}, 10 \times 10\mathrm{mm}^2, \mathrm{IR} = 40\,\mathrm{mm}$

Field Reference B_{coil}

$$\text{Shielding Factor} = \frac{B_{\mathrm{coil}}}{B}$$

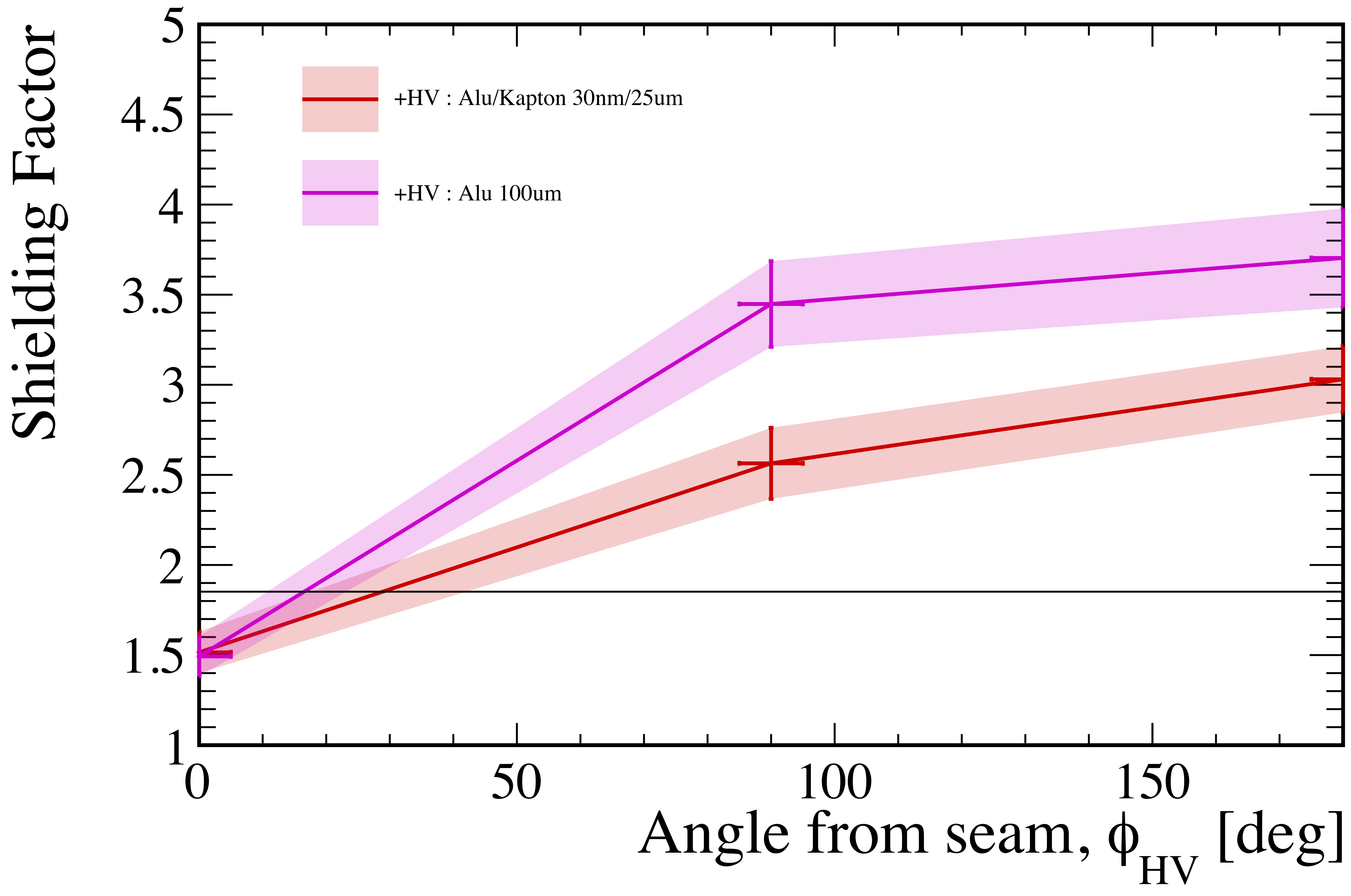

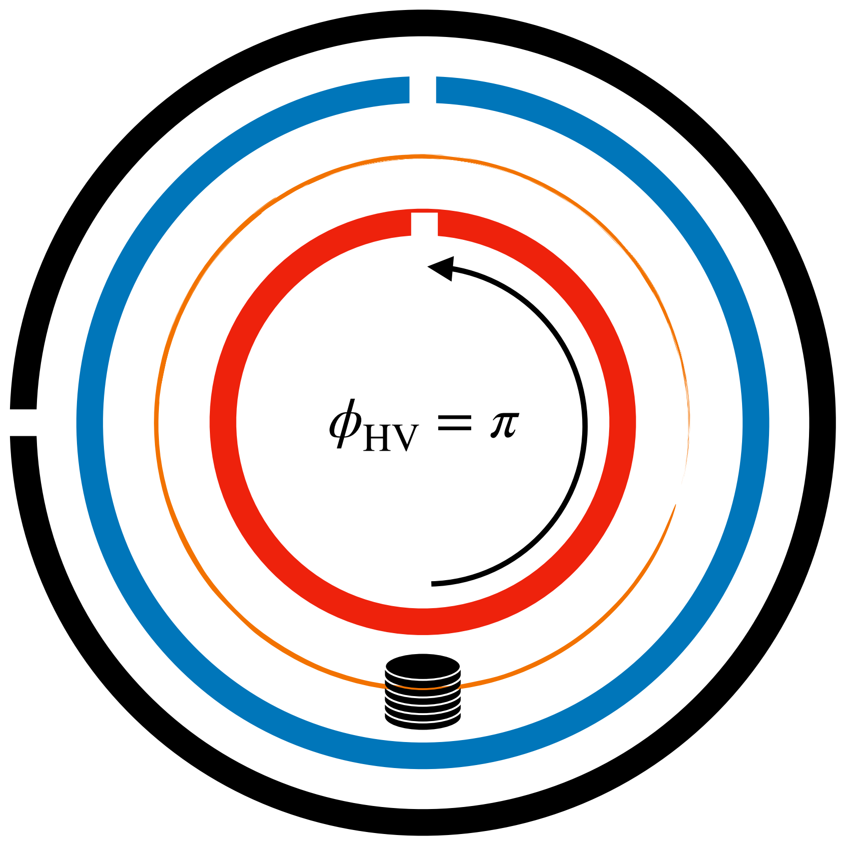

$\mathrm{PulseCoil}: \mathrm{Alu}, 10 \times 10\mathrm{mm}^2, \mathrm{IR} = 40\,\mathrm{mm}$

GND : Alu/Kapton 30 nm

HV : Alu/Kapton 30 nm

Radial Magnetic Field Measurements

- Measured using a pickup coil ( ) at radius $30.0 \pm 0.5\,\mathrm{mm}$, close to the muon orbit radius.
- Different components added to observe effect, due to induction of eddy currents.

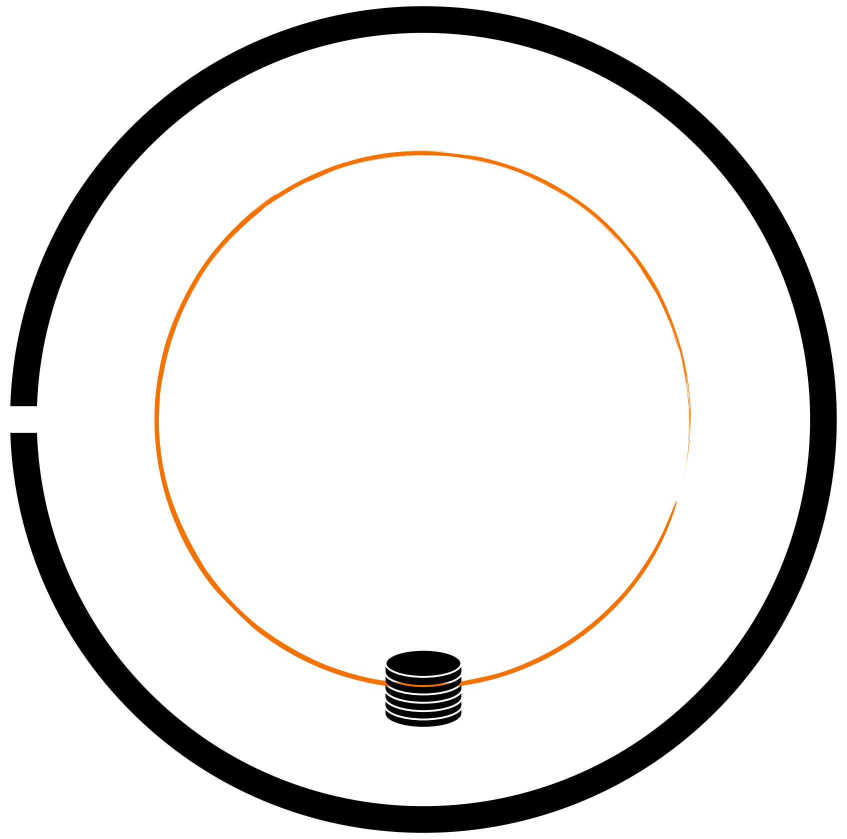

$\mathrm{PulseCoil}:\ \mathrm{Alu}, 10 \times 10\mathrm{mm}^2, \mathrm{IR} = 40\,\mathrm{mm}$

Field Reference B_{coil}

$$\text{Shielding Factor} = \frac{B_{\mathrm{coil}}}{B}$$

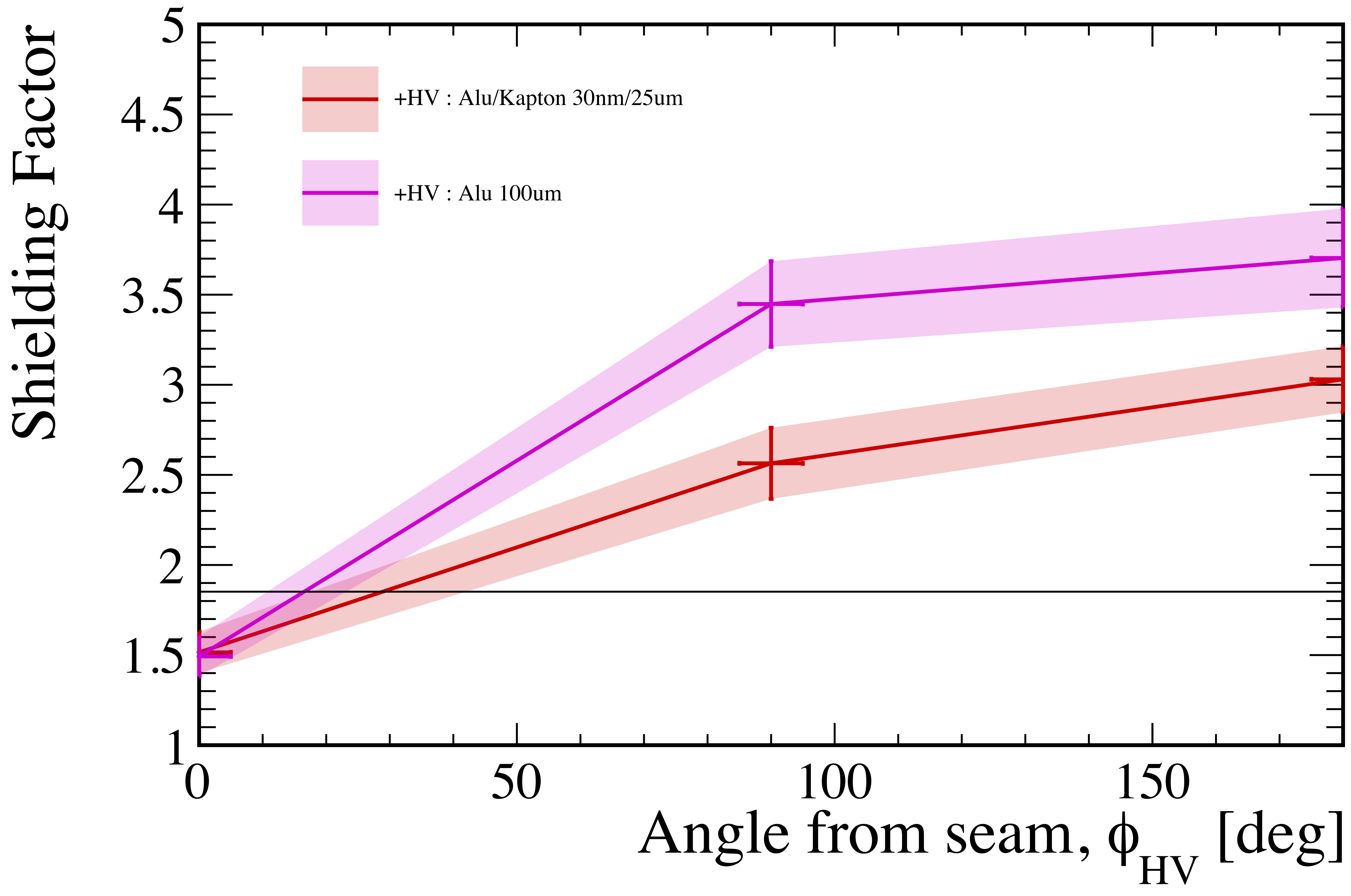

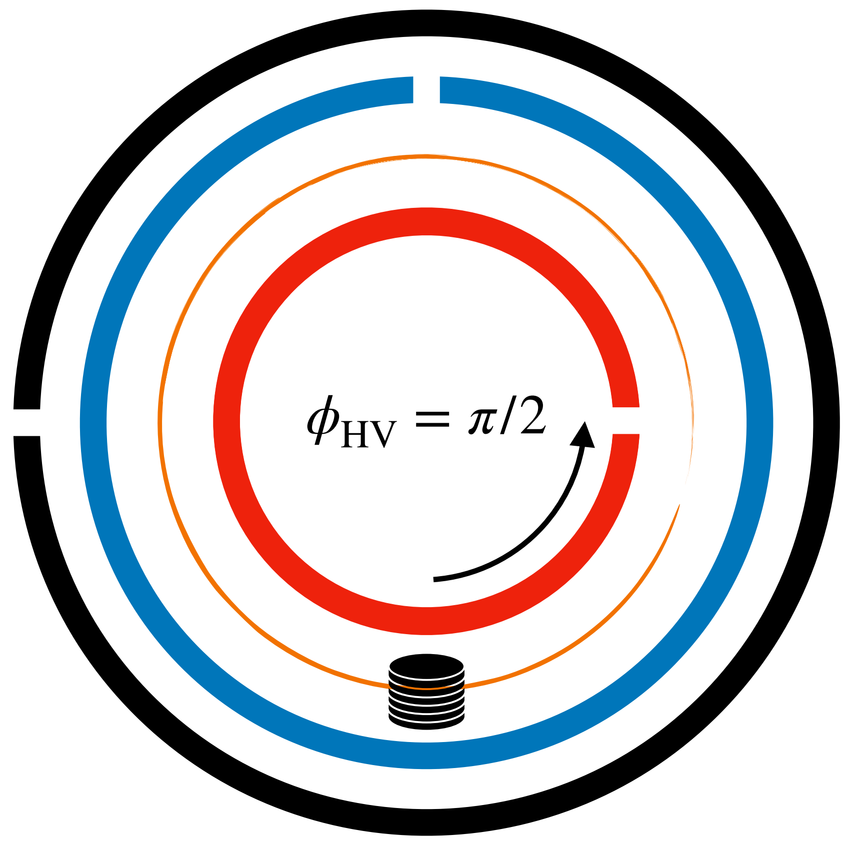

$\mathrm{PulseCoil}:\ \mathrm{Alu}, 10 \times 10\mathrm{mm}^2, \mathrm{IR} = 40\,\mathrm{mm}$

GND : Alu/Kapton 30 nm

HV : Alu/Kapton 30 nm

Radial Magnetic Field Measurements

- Measured using a pickup coil (coil symbol) at radius $30.0 \pm 0.5\,\mathrm{mm}$, close to the muon orbit radius.
- Different components added to observe effect, due to induction of eddy currents.

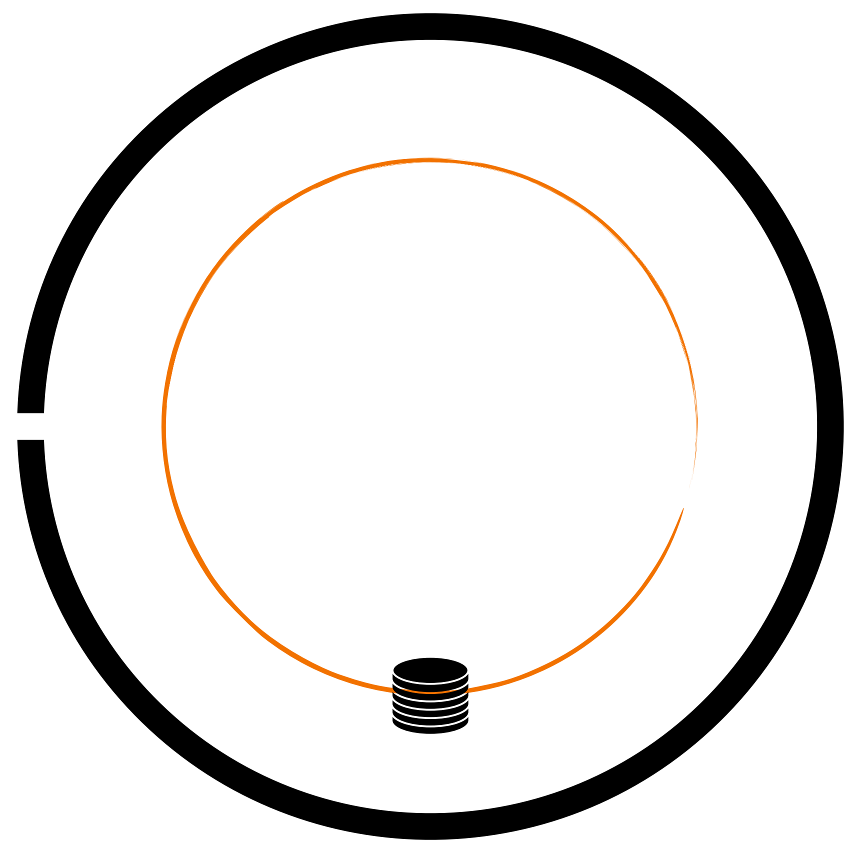

$\mathrm{PulseCoil: Alu, 10 \times 10 mm^2, IR = 40\,mm}$

Field Reference B_{coil}

$$\text{Shielding Factor} = \frac{B_{\mathrm{coil}}}{B}$$

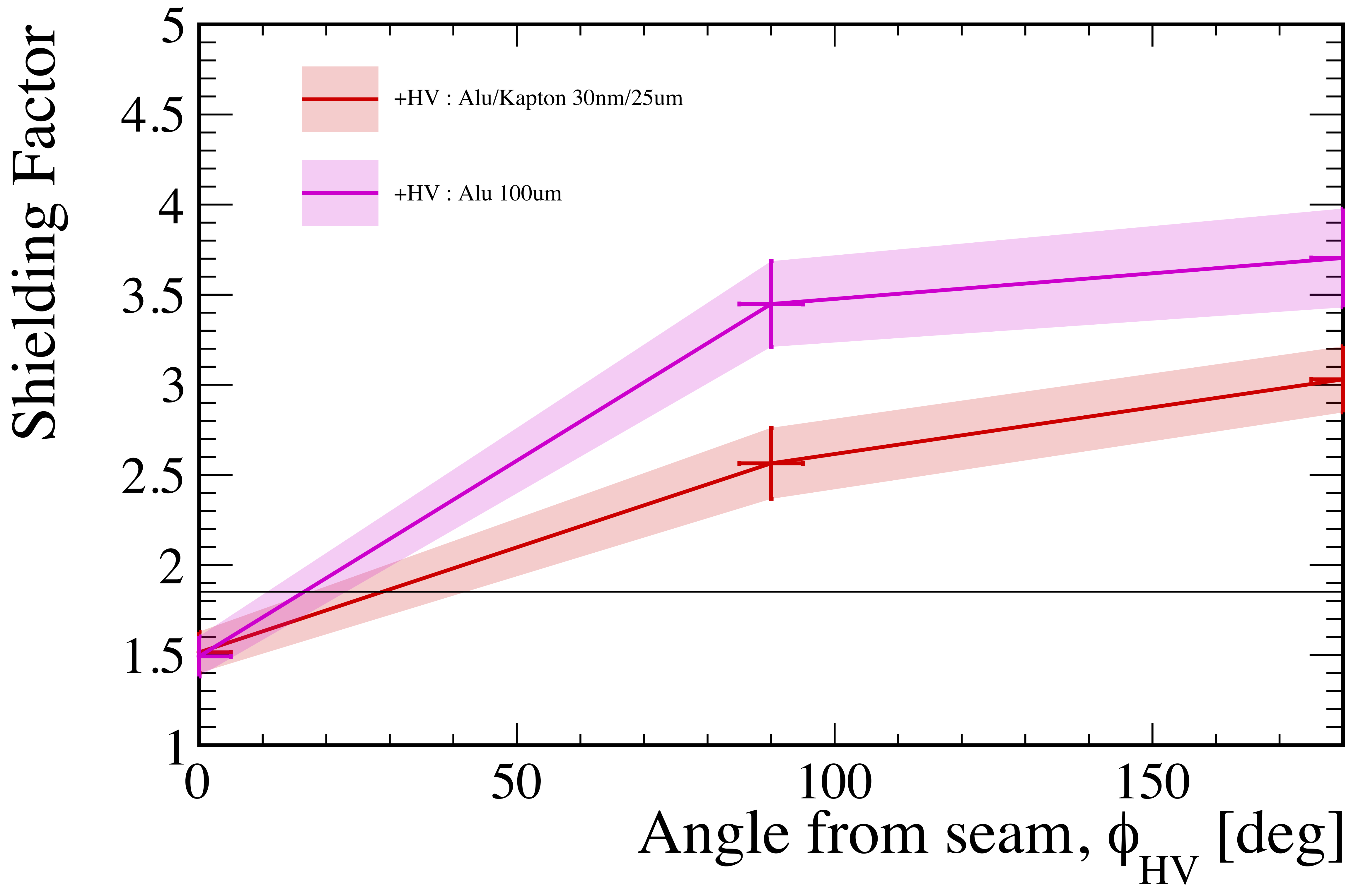

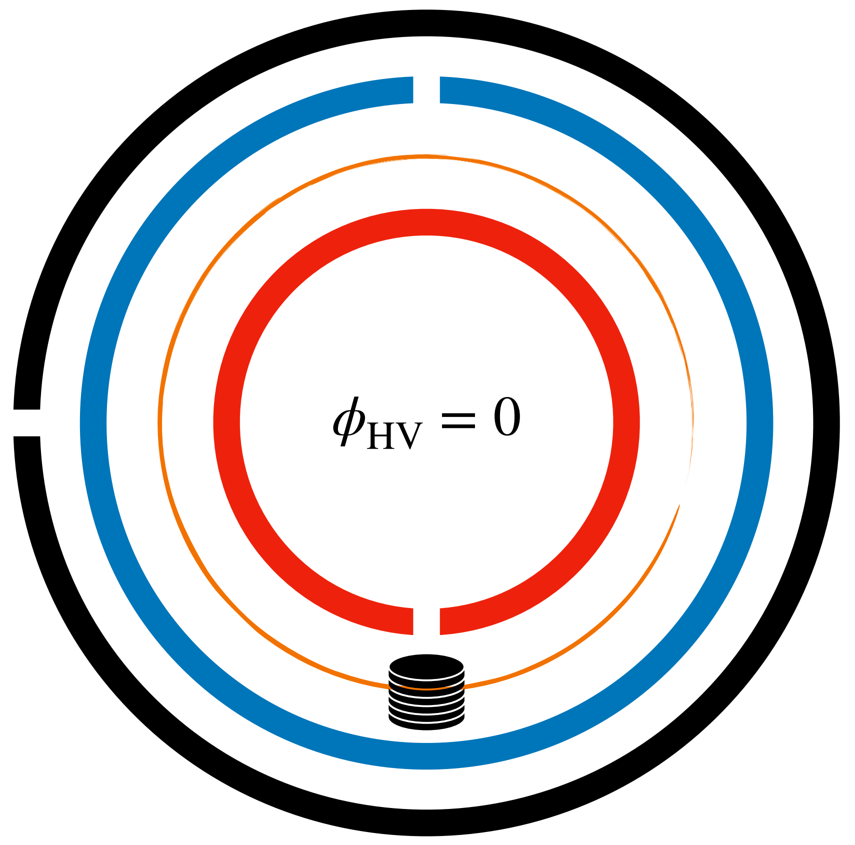

$\mathrm{PulseCoil: Alu, 10 \times 10 mm^2, IR = 40\,mm}$

$\mathrm{GND: Alu/Kapton\ 30\,nm}$

$\mathrm{HV: Alu/Kapton\ 30\,nm}$

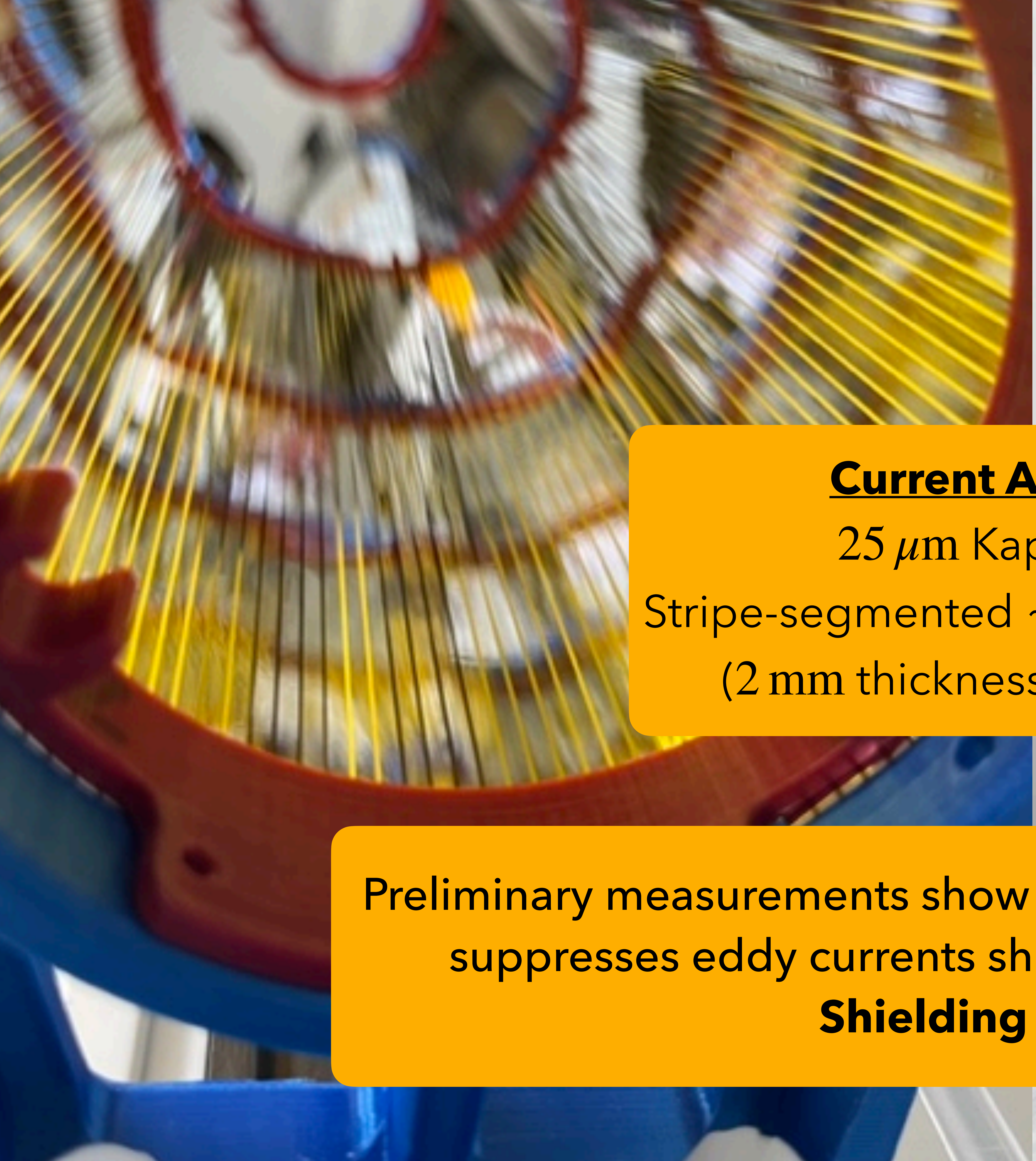

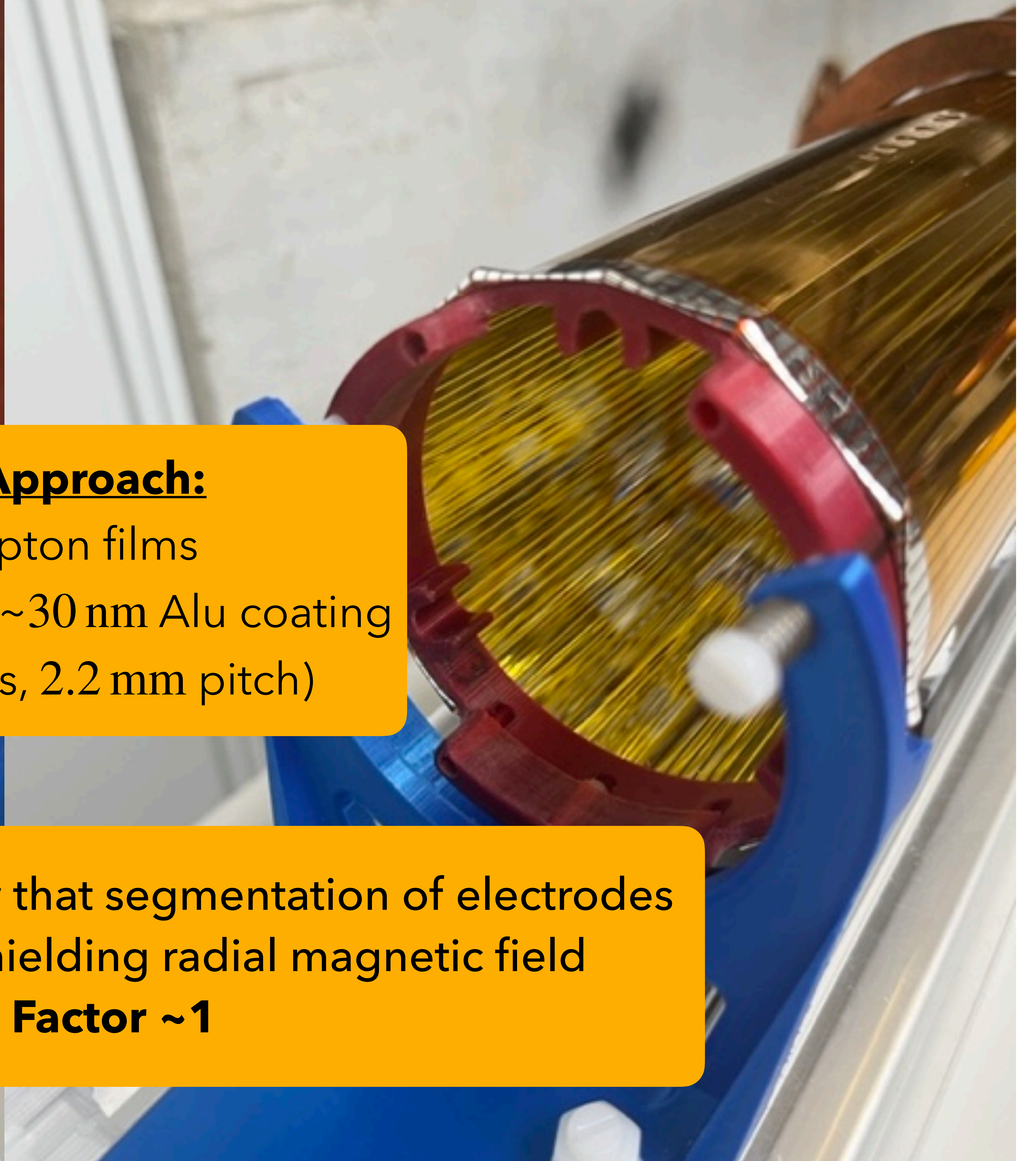

<u>Current Approach:</u>

25 μm Kapton films

Stripe-segmented ~30 nm Alu coating

(2 mm thickness, 2.2 mm pitch)

Preliminary measurements show that segmentation of electrodes suppresses eddy currents shielding radial magnetic field

Shielding Factor ~1

Summary

- We are designing and testing systems to deliver a frozen-spin muon trap comprising:
    - Pulse coils for muon storage
    - Weakly-focusing coil for axial confinement
    - Cylindrical electrodes to satisfy the frozen-spin condition
- The pulse coil circuit must have low inductance to meet the stringent timing requirements: rapid triggering and short width.
- The electrodes must be thin, robust and precisely aligned.
- Segmented electrode geometry considerably reduces the shielding of the pulsed field due to eddy currents.

Thanks to all contributors to the muEDM Experiment

…with thanks in particular to everyone involved in prototype development related to the frozen-spin implementation:

F. Barchetti[1], R. Senn[1]

R. Chakraborty[1], A. Doinaki[1,2], C. Dutsov[1], K. Michielsen[1,2] ,D. Sanz-Becerra[1]

K. Kirch[1,2], P. Schmidt-Wellenburg[1]

1) Paul Scherrer Institute; 2) ETH Zürich;

Project funded by

Schweizerische Eidgenossenschaft
Confédération suisse
Confederazione Svizzera
Confederaziun svizra

Swiss Confederation

Federal Department of Economic Affairs, Education and Research EAER
State Secretariat for Education, Research and Innovation SERI

Muon Electric Dipole Moment

A permanent EDM requires T violation, equivalently CP violation.

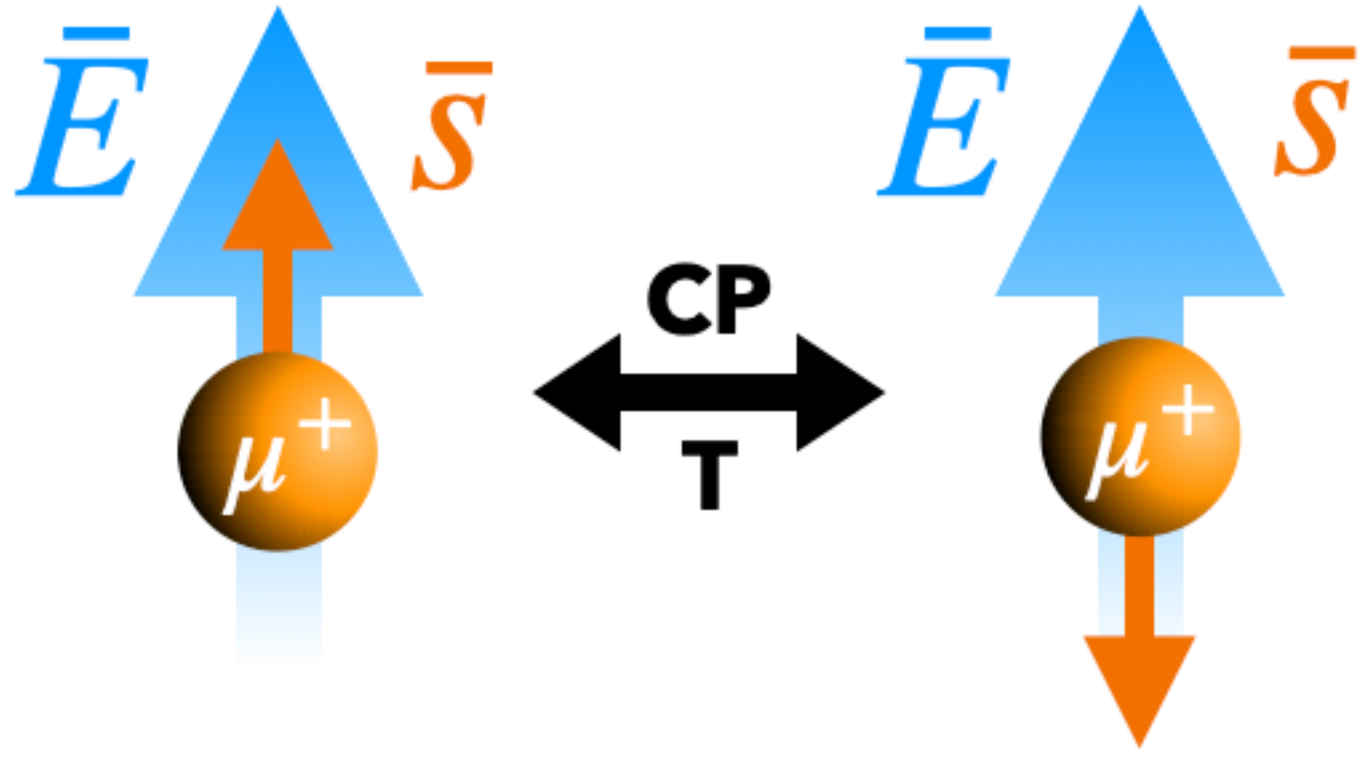

$$H_\mu^{EDM} \overset{\beta\to 0}{\propto} d_\mu \bar{\sigma}\cdot\bar{E}$$

Hamiltonian EDM term is CP violating

$d_\mu \leq 1.8\times 10^{-19} e\,.\,\mathrm{cm}$ (95 % C . L.)
(Muon g-2 Collaboration, 2009)

SM Prediction: $d_\mu^{SM} = 1.4\times 10^{-38}\, e\,.\,\mathrm{cm}$
(Yamaguchi & Yamanaka, 2020)

$d_e \leq 4.1\times 10^{-30} e\,.\,\mathrm{cm}$ (Roussy et al., 2023) $\overset{LFU}{\Longrightarrow}$? $d_\mu \leq \frac{m_\mu}{m_e} d_e = 6.0\times 10^{-28} e\,.\,\mathrm{cm}$

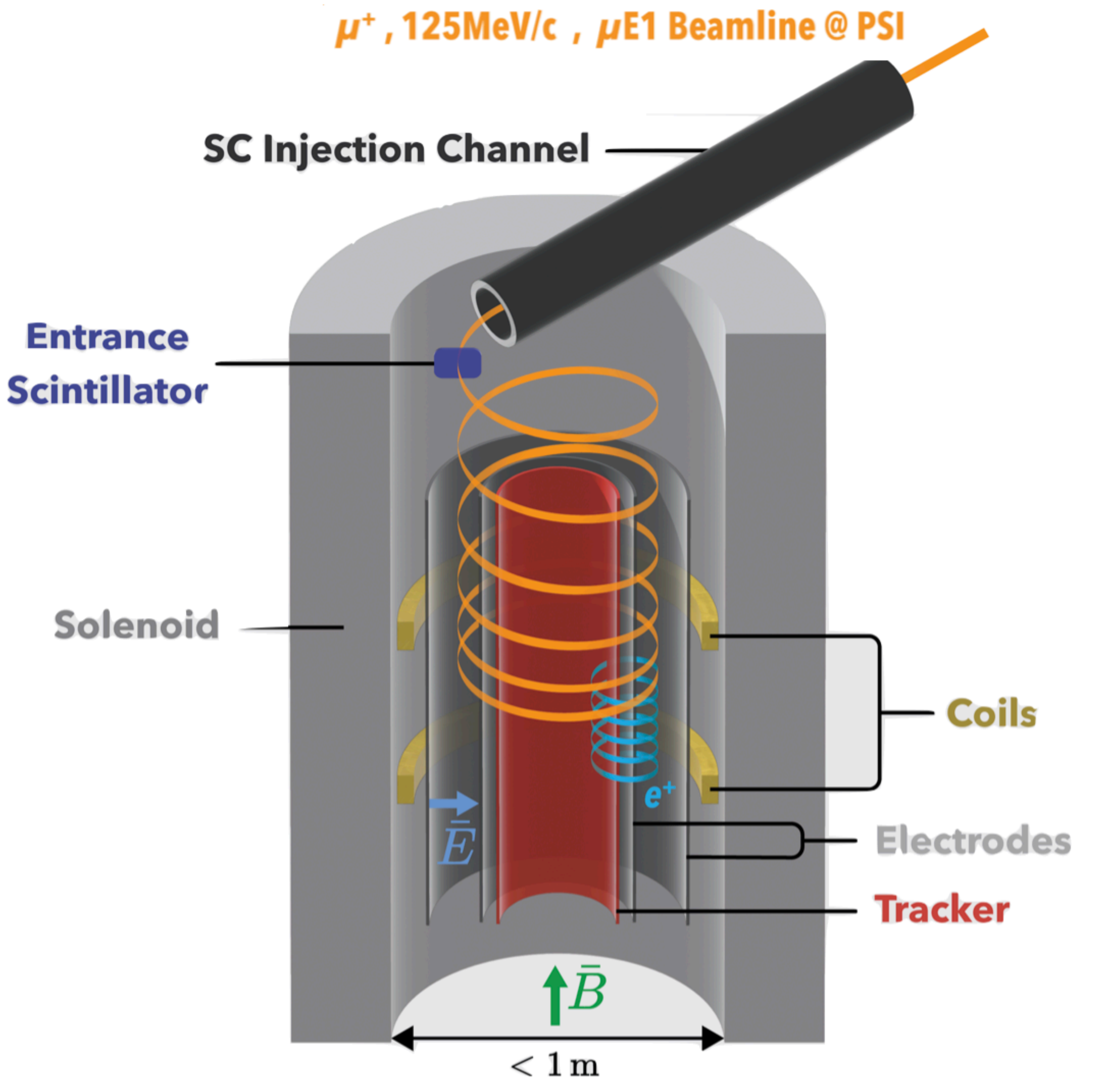

$$\sigma(d_\mu) = \frac{\hbar}{2c\tau_\mu}(\beta\gamma\bar{\alpha}P_0 B\sqrt{N})^{-1}$$

Polarisation $P_0 \approx 0.95$

Eff. Decay Asymmetry $\bar{\alpha} \approx 0.3$

Solenoid Field $B = 3\,\mathrm{T}$

Phase I	Phase II
πE1 Beamline:	μE1 Beamline:
$p_\mu = 28\,\mathrm{MeV}/c$	$p_\mu = 125\,\mathrm{MeV}/c$
$\gamma = 1.03$	$\gamma = 1.54$
$\dot{N}_\mu = 4\times 10^6 \mu^+/s$	$\dot{N}_\mu = 1\times 10^8 \mu^+/s$
$\dot{N}_e = 0.25\, e^+/\mu^+ \cdot 0.0005 \cdot \dot{N}_\mu$	$\dot{N}_e = 0.25\, e^+/\mu^+ \cdot 0.0036 \cdot \dot{N}_\mu$
(Storage rate $2\,\mathrm{ms}^{-1}$)	(Storage rate $360\,\mathrm{ms}^{-1}$)
$\sim 2\times 10^{-21} e\,.\,\mathrm{cm}$	$\sim 6\times 10^{-23} e\,.\,\mathrm{cm}$

(with $N \leftrightarrow$ 200 days)

Y. Yamaguchi & N. Yamanaka. *PRL*, 125:241802, 2020. DOI: 10.1103/PhysRevLett.125.241802.
A. Adelmann *et al*. 2021. arXiv: 2102.08838 [hep-ex]
G. Bennett *et al*. *PRD*, 80:052008, 2009. DOI: 10.1103/PhysRevD.80.052008
T.S. Roussy et al. Science, 381(6653):46–50, 2023. DOI: 10.1126/science.adg4084

Frozen Spin Technique

Goal: Configure E, B fields such that spin follows velocity vector and EDM is the only inherent source of relative spin precession.

$$\frac{\mathrm{d}\bar{\beta}}{\mathrm{d}t} = \bar{\Omega}_c \times \bar{\beta} \qquad \frac{\mathrm{d}\bar{s}}{\mathrm{d}t} = \bar{\Omega}_0 \times \bar{s}$$

$$\bar{\Omega} = \bar{\Omega}_0 - \bar{\Omega}_c = \frac{aq}{m}\left(\bar{B} - \frac{\gamma}{\gamma+1}(\bar{\beta}\cdot\bar{B})\bar{\beta} - \left(1 + \frac{1}{a(1-\gamma^2)}\right)\frac{\bar{\beta}\times\bar{E}}{c}\right) + \frac{\eta q}{2m}\left(\bar{\beta}\times\bar{B} + \frac{\bar{E}}{c} - \frac{\gamma/c}{\gamma+1}(\bar{\beta}\cdot\bar{E})\bar{\beta}\right)$$

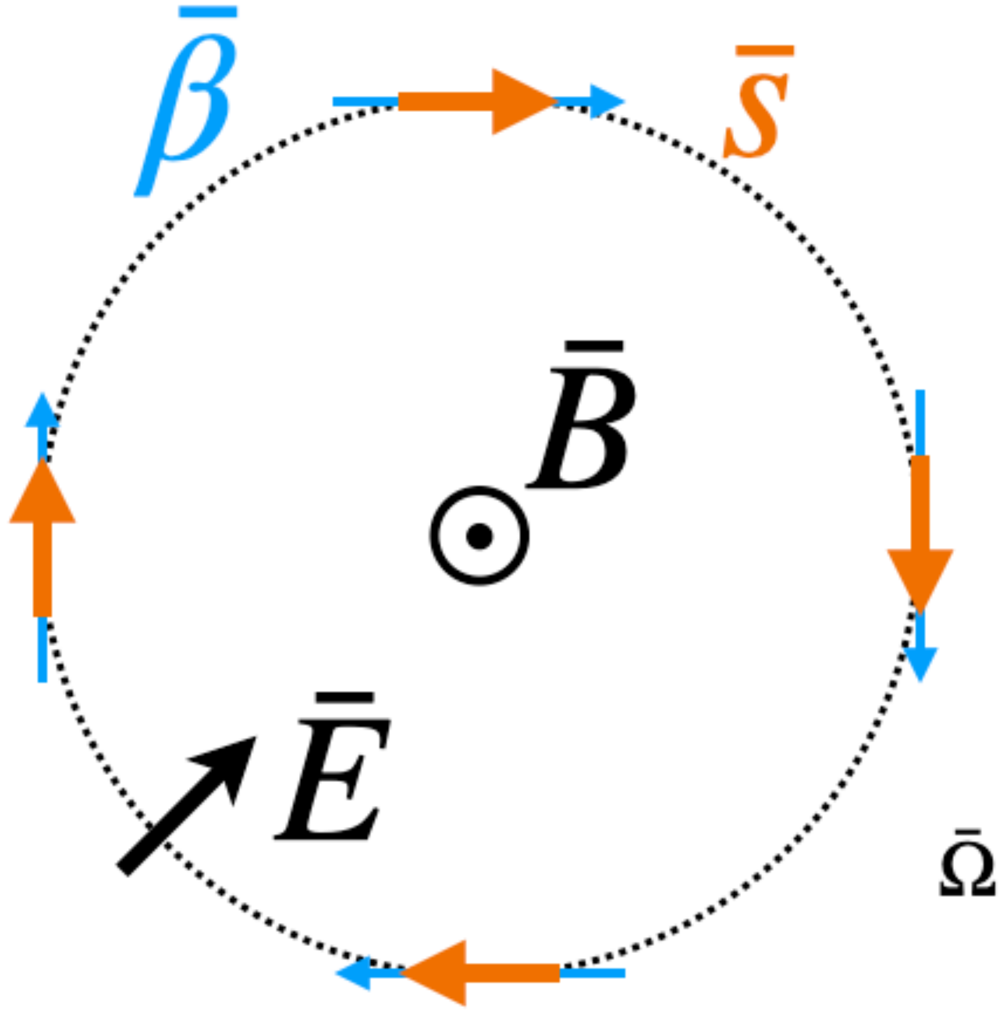

$$\text{Frozen Spin Condition}: \; E_f \overset{a<<1}{\approx} aB\beta c\gamma^2$$

$$\bar{\Omega} = \frac{\eta q}{2m}\left(\bar{\beta}\times\bar{B} - \frac{\bar{E}}{c}\right) \quad \text{for} \quad |\bar{E}| = E_f \quad , \quad \bar{\beta}\cdot\bar{E} = \bar{\beta}\cdot\bar{B} = \bar{E}\cdot\bar{B} = 0$$

Experimental Requirements:

1. Fields ⊥ Velocity
2. Precisely tuned $E = E_f$
3. Constrained B_r (radial), E_z (axial)

Any periodic deviations must be stable over the timescale of τ_μ.

Pulse Generator Simulation

- A circuit model of a pulse generator has been developed in LTSpice with passive pulse shaping and damping of after-pulse oscillations.
- This provides input to storage simulations studying storage efficiency and systematic effects, as well as informing constraints on the electrical properties of the pulse coils.

LTSpice Simulation (T. Hume & P. Schmidt-Wellenburg, PSI)

Split-Quadrant Coil

- Current investigation: determine whether synchronisation of pulses into each quadrant can provide an advantage by lowering the inductance.
- This introduces some additional challenges:
  - More complex circuit for supply and characterisation
  - Strong inductive couplings (mutual inductance)

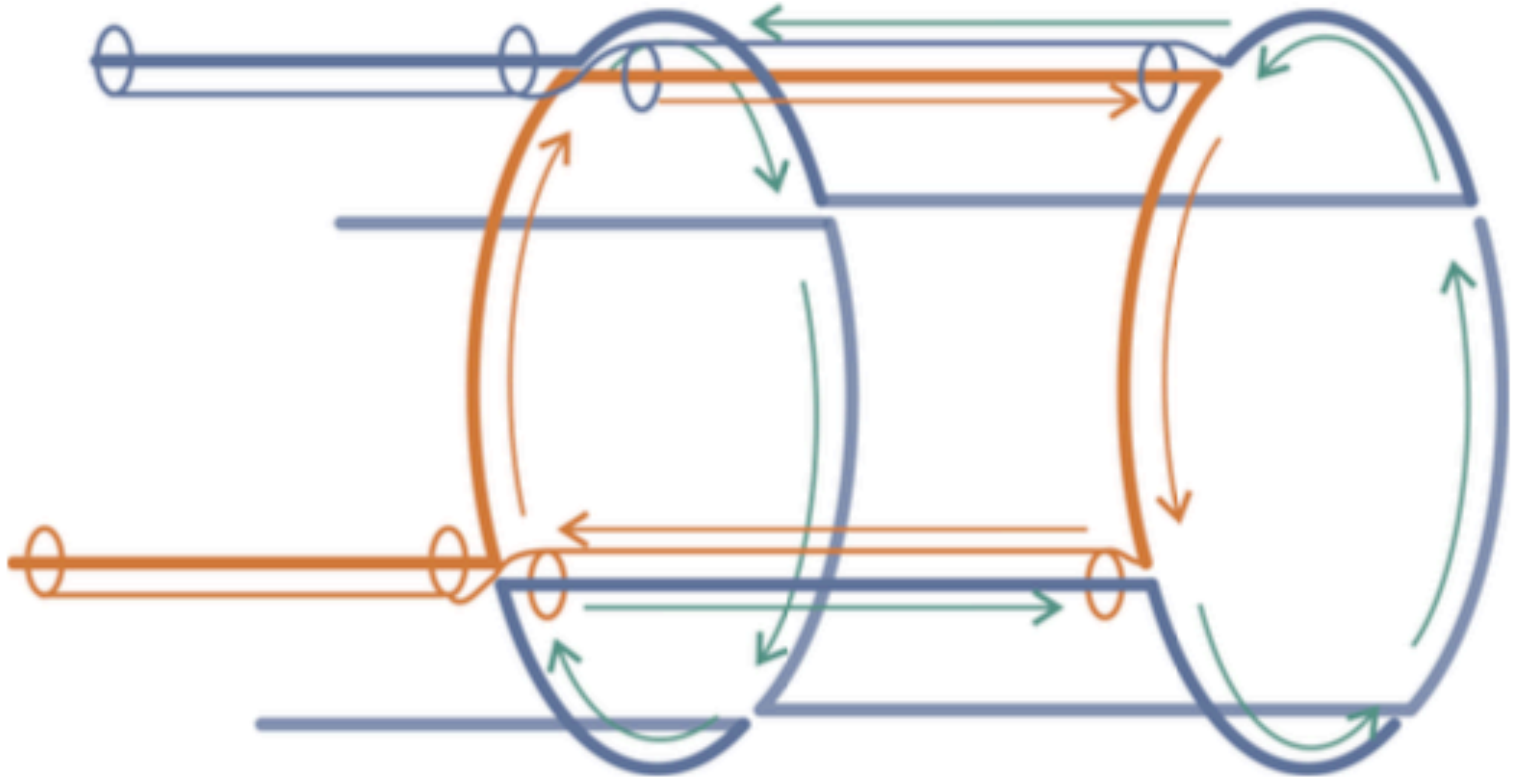

Circuit Schematic, 4 parallel pairs (P. Schmidt-Wellenburg, PSI)

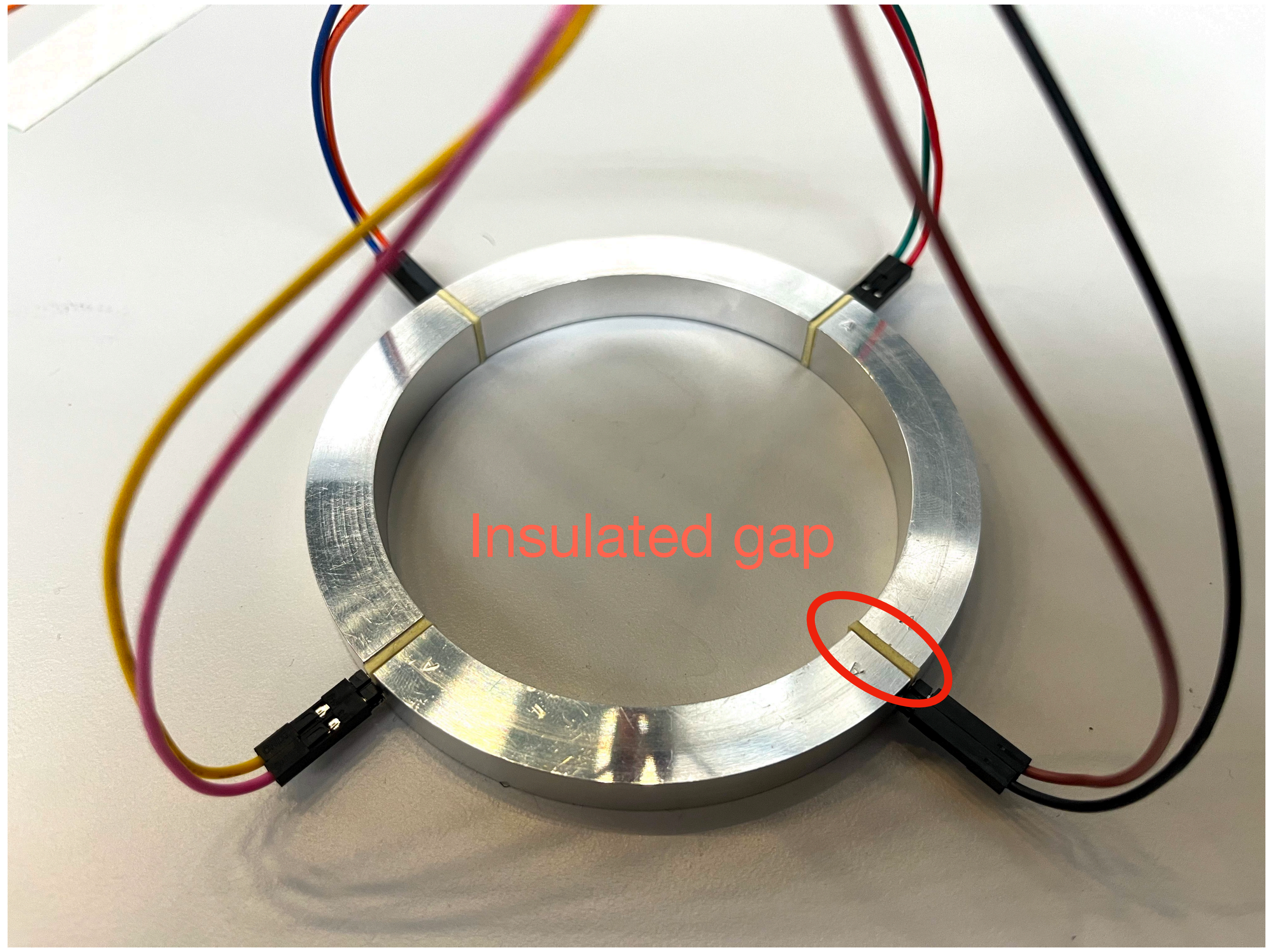

Ansys / LTSpice Simulations:

$$L_{quad} \rightarrow \frac{L_{coil}}{2}$$

$$L_{quad,par8} \rightarrow \frac{L_{coil}}{10}$$

(Ideal parallel supply of 8 quadrants would be 1/16, neglecting couplings)

Outlook

	Design Optimisation	Field Characterisation
Storage Pulse B Field	Supply split quadrants of coils with synchronised pulses to lower total L	Produce calibrated pickup coil to map radial field strength
Frozen-spin E Field	Individual wire strands may facilitate more precise alignment	Surface profiling based on reflected laser line image

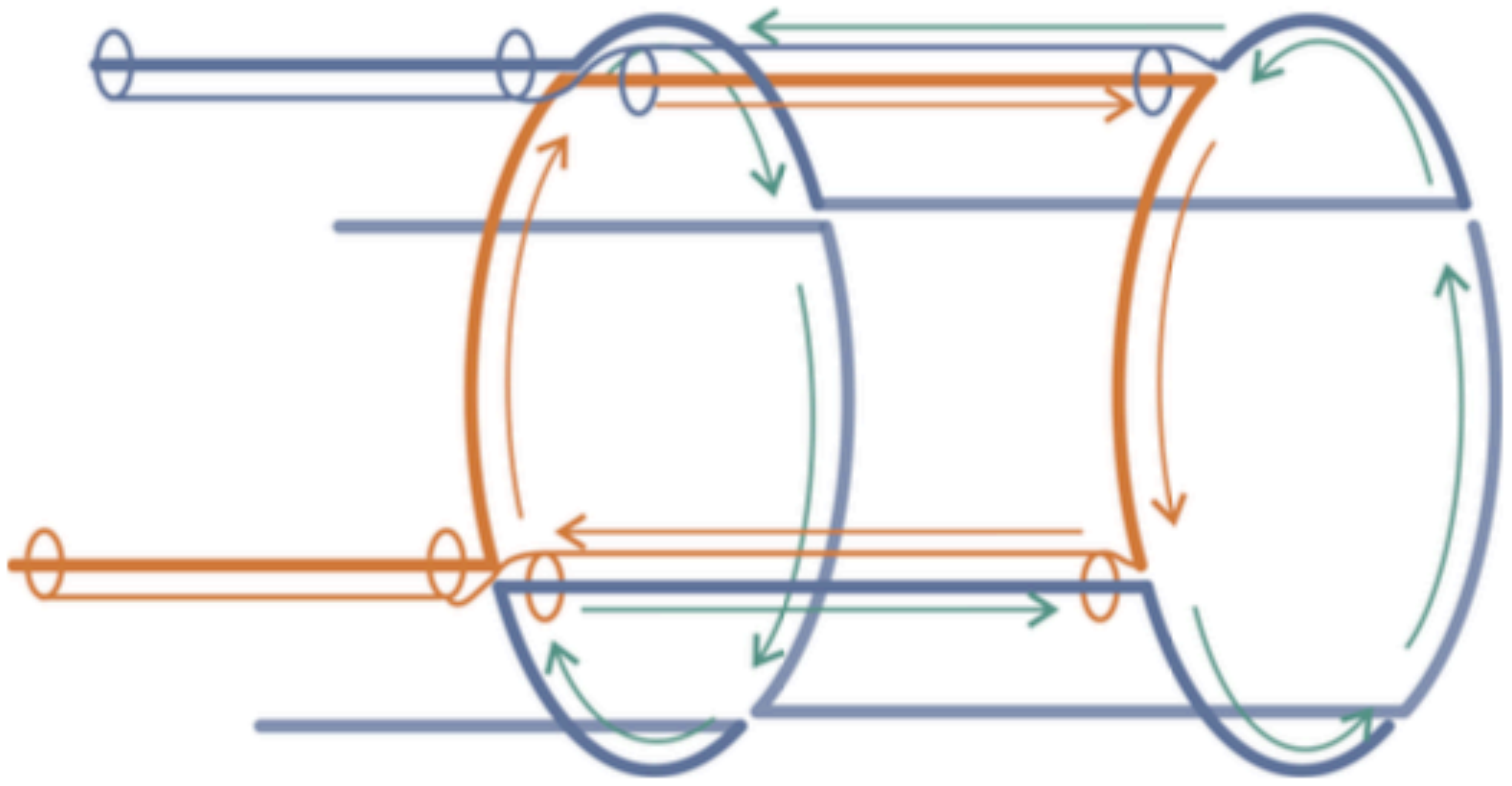

Circuit Schematic, 4 parallel pairs (P. Schmidt-Wellenburg, PSI)